TENTATIVE SEISMIC DESIGN GUIDELINES FOR ROCKING STRUCTURES

Trevor E. Kelly[1]

SUMMARY

Many new and existing buildings have insufficient weight to resist overturning loads due to earthquakes without uplift. Previous versions of the New Zealand loadings code allowed simplified procedures for the design of rocking structures provided the ductility factor was limited to not more than two. The new loadings code, NZS 1170.5, removed this exemption and requires that a special study be performed whenever energy dissipation through rocking occurs. This paper presents a tentative design procedure intended to substitute for the special study required by the code.

The resistance function of rocking walls was developed from the principles of engineering mechanics. The results from a series of time history analyses were used to develop a procedure to estimate maximum seismic displacements and empirical equations were derived to estimate the dynamic amplification of inertia forces. A substitute structure approach, using spectral displacements at an effective period calculated from the ductility factor, provided accurate predictions of the displacements from more sophisticated nonlinear analyses.

Four example designs were completed and the predicted response compared to time history results. The procedure provided a satisfactory estimate of response for regular structures, but it was less accurate where torsional effects were significant.

1. INTRODUCTION

Many new and existing buildings have insufficient self weight to resist overturning loads expected during earthquakes without uplift of structural elements. Uplift can be prevented by the use of tension piles, but these add significant costs and may impose larger loads on the structure above. Observed and analytical evidence suggests that local uplift and rocking will not be detrimental to seismic performance and in fact may be beneficial in limiting forces transmitted into the structure [3]. In fact, rocking systems have been implemented as an effective isolation system in New Zealand and worldwide [4].

Uplift is a nonlinear phenomenon in that the foundation changes state from full contact with the subsoil to partial contact. Because of this nonlinearity the structural deformations, and the associated redistribution of forces, cannot be quantified using conventional linear elastic analysis. Pioneering work in the development of design procedures for rocking structures was published in NZ in 1978 by Priestley, Evison and Carr [5] and this has been used as a basis for published guidelines such as FEMA 356 [6]. However, subsequent research suggests that there are limitations in these procedures which have prevented their widespread application [7]. This paper summarises a research project funded by the EQC Research Foundation [8] to develop design guidelines to enable designers to quantify the effects of rocking on structures without performing a nonlinear analysis.

1.1 Code Requirements

For designs performed in New Zealand to the provisions of the loadings code which applied through 2005, NZS4203:1992 [1], uplifting structures were governed by Clause 4.11.1.2 which stated that:

> *Where dissipation of energy is through rocking of foundations, the structure shall be subject to a special study, provided that this need not apply if the structural ductility factor is equal to or less than 2.0.*

In practice, this exclusion was interpreted by designers as rocking structures would require no special design provisions provided that uplift occurred at a level of seismic load no less than 50% of the full elastic load. Many low-rise shear wall buildings met this restriction and were designed to rock under the code specified seismic loads.

NZS 1170.5:2004 [2], which replaces NZS4203, addresses rocking structures in Section 6.6 which requires that:

> *Where energy dissipation is through rocking of structures…, the actions on the structure shall be determined by a special study.*

A special study, in terms of NZS 1170, requires the development of a computer model of the structure and an assessment of the time history of response of the structure to a suite of probable earthquake motions. This type of analysis requires specialised software and a level of expertise which most design offices cannot provide.

While special studies are justified for large and important structures, the majority of structures where uplift may occur are of such scope that the cost of the special study, and the time required, is prohibitive. For these buildings, anecdotal evidence suggests that many designers are allowing rocking to occur by default without quantifying the effects, due to an absence of guidelines to evaluate these effects within a design office environment.

The alternative to permitting rocking, which is to prevent rocking by the use of massive foundations or tension piles, leads to added expense and additional loads to the structure above. For the retrofit of earthquake prone buildings, new foundations to resist uplift often form the major cost item and these costs are often so prohibitive that the owner is discouraged from attempting a seismic upgrade. Guidelines for the design of new rocking elements to improve the seismic

[1] *Technical Director, Holmes Consulting Group, Auckland (Member)*

resistance of existing buildings will result in more cost effective retrofits and encourage the continued safe usage of our building stock.

1.2 Previous Research

The dynamics of rocking blocks have been described comprehensively in the literature (see for example references [9] to [14]) and are not repeated here. These references generally show that the response of rocking systems is best described by solving the second order ordinary differential equation based on the rotational moment of inertia of the block, with the dynamics of the system described by the block angular velocity. The energy loss of the system is replicated using an apparent coefficient of restitution approach first developed by Housner [9].

The original work on rocking systems by Housner was later extended by a number of researchers, including Yim, Chopra and Penzien [10], Ishiyama [11] and Psycharis [12] as well as the researchers in New Zealand noted previously [5]. Experimental work such as the uplifting frame studied by Huckelbridge [3] demonstrated the potential benefits of allowing partial uplift.

More recently, extensive experimental and analytical work at the University of Auckland by Ma, ElGawady and others, [13, 14], has extended our knowledge of aspects of rocking and methods of evaluating rocking response. This will result in a better understanding of the dynamics of rocking and the influence of factors such as the aspect ratio and interface material. In the medium to long term, this research will result in much more sophisticated tools to evaluate rocking structures.

Most of the rocking block research referenced above assumes a rigid block on a rigid foundation. For uplifting structures, soil interaction is important and the potential for soil yielding must be considered. This is a complex topic and work in this area is not yet developed sufficiently for design office use. Progress is being achieved, as shown by research in New Zealand [15, 16] and internationally [17, 18, 19]. As this basic research is progressed it will be possible to extend design office procedures to include these important effects.

A Canadian study [20] evaluated the effect of foundation rocking on shear walls and recommended that footings need not be designed for ductility factors less than 2. Ironically, the impetus for this study was the draft NZ code DR00902, an earlier version of NZS1170 which contained a provision similar to that in NZS4203. This provision was omitted when the draft progressed into the final version, resulting in the need for these guidelines. The Canadian study related to walls 7 to 30 stories high, where the current study considers walls up to 6 stories. The Canadian study focused on the effects of uplift on drift but not on dynamic amplification of forces and so it is not directly applicable to the objectives of this project.

1.3 Rocking and Uplift

Most research referenced above relates to classical rocking structures, which are rigid blocks on rigid foundations. These structures rock as the reaction switches from one corner of the block to the opposite corner. The direction of the restoring moment provided by the self weight alternates each time the reaction changes from one corner to the other.

The engineered structures which are the subject of this paper differ from rocking blocks in that they rest on flexible foundations. Under seismic excitation rocking is enabled through the separation of a part of the foundation from the supporting soil. As the load reverses, the uplifted portion of foundation reverts to contact with the subsoil and the opposing end starts to separate. A typical structural model for this type of structure is an elastic foundation modelled by a bed of tension only springs, also known as a Winkler model [17].

Structures termed variously rocking or uplifting are more accurately characterised as uplifting systems, as they have no tension attachment to the ground but do have more than two support points. Typically more than one support point is active at any point in the rocking cycle. Examples of uplifting structures are shear walls where only a portion of the wall separates from the ground or a frame elevation with more than two columns where only the end column uplifts. This is the type of system which is the subject of this project. As the soil springs become stiffer, representing progressively stiffer foundation material (clays and gravels to rock for instance), the wall response approaches that of a rigid uplifting block.

1.4 Development of Guidelines

Many of the characteristics of uplifting walls can be developed using standard design office procedures and the principles of engineering mechanics. These include the assignment of properties to soil springs; foundation pressure; lateral load to initiate rocking and the period of the rocking structure. Procedures to develop these properties are described in the following section.

The dynamic characteristics of an uplifting wall are more complex because of the nonlinearity presented as the foundation separates from the ground. To develop these characteristics, a series of analytical studies on various wall configurations was performed. The analyses were intended to represent examples of special studies in terms of current design office practice, rather than research practice. The aim was to develop methods to estimate the results of this type of special study without doing a time history analysis of a specific structure. In particular, the goal was to develop procedures to estimate:

1 Maximum displacements at the top of the rocking structure.

2 The pressure on the sub-structure during rocking.

3 The distribution of forces in the structure due to rocking if different from the non-rocking distributions.

The dynamic response of rocking blocks exhibits complex behaviour and it is likely that ongoing research will provide a better understanding of the dynamics of rocking structures and ways to incorporate rocking into design.

This study is an interim attempt to quantity the response with sufficient certainty appropriate for design office use. The guidelines are developed using procedures which would typically be used for a “special study” but are not fully rigorous as they do not fully quantify impact effects, nonlinear soil properties, radiation damping, etc.

2. ENGINEERING MECHANICS FORMULATION OF ROCKING WALLS

2.1 Soil Springs

For structural walls the foundation material is often more flexible than the wall itself. This is especially true for squat walls which are likely to be designed using these guidelines. Accurate representation of the dynamic characteristics of the structure requires that the foundation flexibility be included by the use of soil springs.

For shallow bearing foundations that are flexible compared to the supporting walls, FEMA 356 [6] provides a design procedure using a Winkler soil model. The distributed vertical stiffness is calculated by dividing the total vertical stiffness by the area. The uniformly distributed rotational stiffness is calculated by dividing the total rotational stiffness of the footing by the moment of inertia of the footing. The procedure reproduced in Figure 1 may be used to decouple these stiffnesses.

This procedure is suited to a design office as the properties can be routinely calculated using a spreadsheet. A set of soil springs is defined by the soil shear modulus, G, and the Poisson's ratio, ν. The spring stiffness values correlate to the equivalent soil stiffness per unit length and they are different for the two end zones and the central portion. The springs in the end zones have a higher stiffness than the central zone. The end zones are defined as extending a distance of B/6 from each end of the wall, where B is the foundation width.

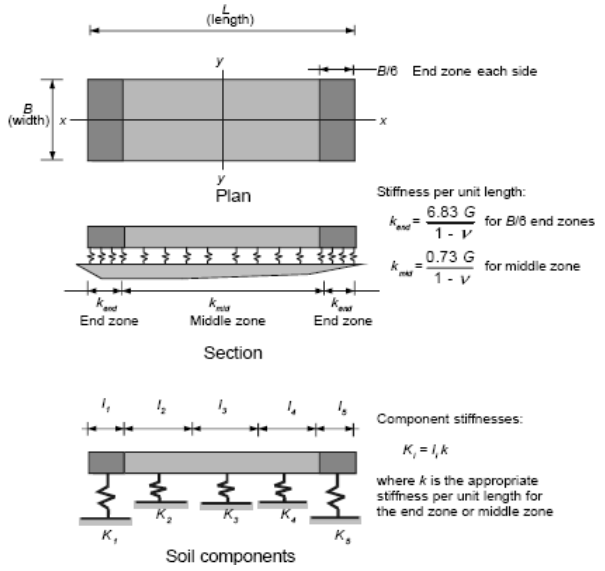

Figure 1. Shallow Footing Model (Reproduced From FEMA 356, Figure 4-5).

2.2 Rocking Mechanism

Under a pseudo-static lateral displacement, a wall will remain stable until the centroid of the wall is beyond the toe of the wall about which rocking occurs, as shown schematically in Figure 2.

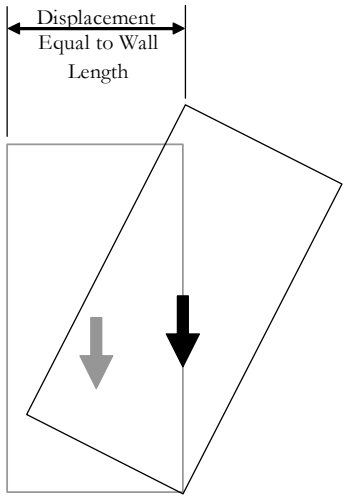

Figure 2. Rocking Block Stability Limit.

The centroid of a wall with a uniformly distributed mass is located at mid-height. Instability occurs when the horizontal displacement at the top of the wall exceeds the wall dimension in the direction of the applied displacement, generally equal to the wall gross length. If a static load sufficient to initiate uplift is applied the wall will start to uplift but will not overturn provided the displacements are less than the stability limit. This characteristic is termed dynamic stability in this paper and is discussed further below.

2.3 Foundation Pressure

For design office calculations, it is generally assumed that at ultimate seismic loads the overturning moment is resisted by a compression stress block, as shown in Figure 3. The stress block is centred at the location of the concentrated reaction, extends to the compression face of the foundation and is symmetric about the reaction point. This configuration is used to develop equations for the effective lever arm to resist uplift in the design procedures presented later in this paper.

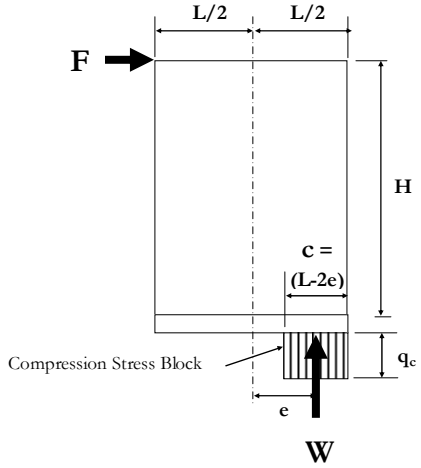

Figure 3. Compression Stress Block Assumption.

2.4 Lateral Load to Initiate Rocking

For a simple rocking block on two springs the lateral load required to initiate rocking can be calculated by equating the overturning moment, FH, to the resisting moment, W(L-c)/2, with both moments taken about the extreme compression edge. This is shown schematically in Figure 4.

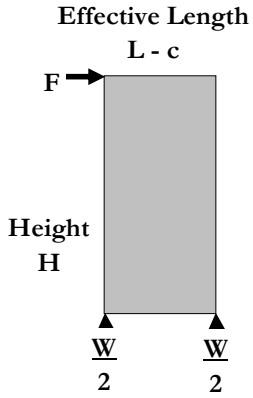

Figure 4. Calculation of Rocking Strength.

This general procedure can be extended to evaluate wall strength for walls with multiple springs, non-planar walls and multiple walls as follows:

1 Obtain the axial forces in each spring by performing a static gravity load analysis. Tabulate these reactions, along

with the coordinates of each spring from a selected reference point about each wall axis.

2 Take moments about each of the two horizontal axes for both positive and negative sense of bending and calculate the position of the centroid.

3 Calculate the resisting moment capacity as the total axial load times the distance to the centroid. The force to initiate uplift is this moment divided by the wall height.

Further adjustments to this procedure are proposed to account for multi-storey walls and they are discussed later in this paper.

2.5 Estimation of Period

If the wall is stiff relative to the soil springs, as will often be the case for squat walls or soft soil conditions, the rocking period can be estimated following a simple procedure summarised in Figure 5.

Table 1 lists the periods calculated from the equations in Figure 5 for a 3.600 m long 3 storey wall on a range of soil springs. For comparison, periods were derived from an equivalent finite element model which assumed a rigid wall. The periods extracted from this model are also listed in Table 1. These results proved that the formula predicted the period from the more sophisticated analysis within 1% for a wide range of soil properties.

As noted, the periods in Table 1 are based on a rigid wall assumption. The example wall has a length of 3.600 m and is 3 stories high so is relatively flexible even when the base is fixed, with a calculated fixed base period of 0.356 seconds.

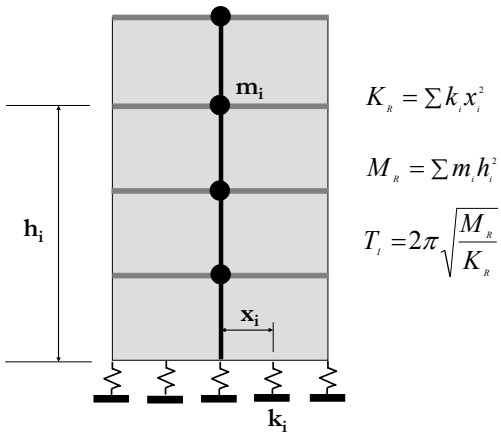

Figure 5. Calculation of Rocking Period.

In Table 2, the results using the formula for the rigid wall model are compared with periods from the flexible wall model. Although the match is reasonable for the soft springs and rigid wall combination, as the soil stiffness increases, or as the relative rigidity of the wall decreases, the error also increases. For the stiffest springs corresponding to set G (Rock) the simplified procedure predicted a period only 55% of the analysis period.

A more accurate rocking period can be predicted in these cases by using the square root of the sum of the squares (SRSS) of the period based on a rigid wall and the period for the fixed base wall (0.356 seconds). The SRSS calculation produced a period within 1% of the model period for all soil spring variations.

Table 1. Comparison of Calculated Periods for Rigid Wall on Springs.

Set	Soil Type	Period Calculated From		Formula / Model
		Formula	Model	
A	Clay Lower Level	4.652	4.614	1.008
B	Clay Mean Level	2.080	2.062	1.009
C	Clay Upper Level	1.471	1.459	1.008
D	Sand & Gravel Lower Level	1.186	1.177	1.008
E	Sand & Gravel Mean Level	0.968	0.961	1.008
F	Sand & Gravel Upper Level	0.839	0.833	1.007
G	Rock	0.237	0.238	0.997

Table 2. Comparison of Calculated Periods for Flexible Wall on Springs.

Set	Period Calculated From		Formula / Model	Wall Period, T_W	SRSS $\sqrt{T_S^2 + T_W^2}$	SRSS / Model
	Formula, T_s	Model				
A	4.652	4.627	1.005	0.356	4.666	1.008
B	2.080	2.093	0.994	0.356	2.111	1.008
C	1.471	1.502	0.979	0.356	1.514	1.008
D	1.186	1.229	0.965	0.356	1.238	1.008
E	0.968	1.025	0.945	0.356	1.032	1.007
F	0.839	0.906	0.926	0.356	0.911	1.006
G	0.237	0.430	0.552	0.356	0.428	0.995
Rigid		0.356				

3. ANALYSIS OF ROCKING WALLS

3.1 Prototype Wall Models

The formulations in the preceding section provide a mechanics based procedure to calculate wall properties including soil spring values; loads to initiate rocking and rocking periods of the wall on flexible foundations. However, it is well known that the response of an uplifting wall to seismic loads is a nonlinear phenomenon and requires an explicitly nonlinear analysis using time integration techniques.

To provide this assessment, an extensive set of single wall models and a limited set of multiple wall models were developed. All analyses were performed using the ANSR-II computer program [21] and full details are provided in [8]. As a summary, the simulation matrix included,

1 A total of 40 single wall configurations encompassing 3 wall lengths (3.600 m, 7.200 m and 14.400 m), ranging between 1 to 6 stories with foundations ranging from soft clay to rock. The periods of the single walls ranged from 0.03 to 3.91 seconds.

2 A combined model, comprising the 3 storey configurations of the 3.600 m and 7.200 m long walls in series, with three foundation stiffness values considered.

3 Two U-shaped walls, the first was 7.200 m x 14.400 m in plan and 3 stories high and the second was 14.400 m x 14.400 m in plan and 2 stories high. Three soil stiffness values were considered for each of the walls.

4 A non-symmetrical wall configuration. This was a two storey square building with 3.600 m long walls on two adjacent elevations and 7.200 m long walls on the other two elevations.

The multiple wall models contained pin ended gravity columns in addition to the walls, as it is shown in Figure 6 for a U-shaped wall and Figure 7 for the non-symmetrical wall.

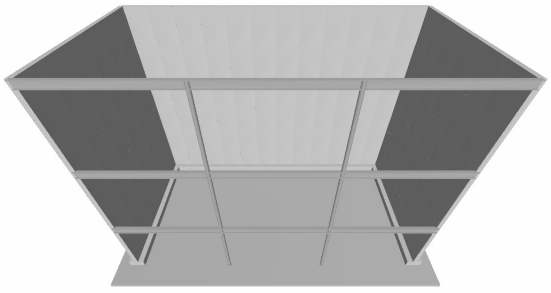

Figure 6. Model of U-Shaped Wall 7.200 m x 14.400 m.

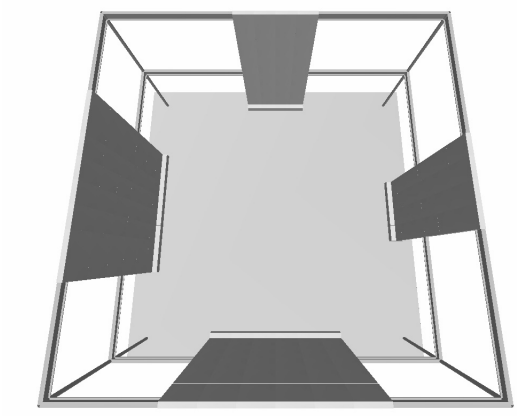

Figure 7. Model of Non-symmetrical Wall Configuration.

3.2 Analysis Models

Each of the basic wall configurations was modelled using a 6 x 6 finite element grid, as shown in Figure 8 for a single three storey wall. The spacings between gridlines were adjusted to fit the different wall lengths and number of stories into the standard 6 x 6 grid. For the multiple wall models, the full structure was assembled from a series of individual walls, each modelled as shown in Figure 8. For these models, soil spring properties were summed at springs common to more than one wall.

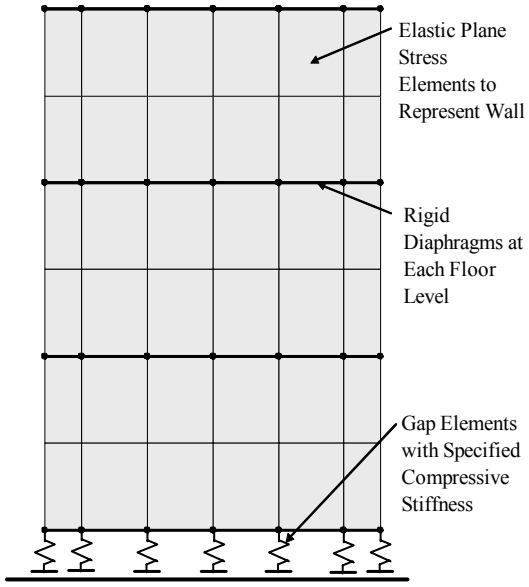

Figure 8. Model Used for Time History Analysis.

Three element types were included in the analysis model as it is shown in Figure 8, and these were,

1 Linear elastic plane stress elements, with properties based on a 200 mm thick concrete wall.

2 Rigid beam elements at each floor level representing a rigid diaphragm. These beams were pinned at each grid intersection. For the three dimensional models a rigid diaphragm formulation was used.

3 Compression only gap elements at each grid intersection between the ground beam and the foundation. The gap elements had compressive stiffness properties representing the different soil types.

In addition to these structural elements, a “dummy” pin ended column element provided second order (P-Δ) effects as the plane stress element formulation did not include geometric stiffness.

The seismic masses were lumped at each floor level and the gravity load was distributed at each nodal point. For the single wall models the total gravity load was half the seismic weight, based on an assumption that the gravity load was shared with two walls in the orthogonal direction.

The computer program based P-Δ effects on the gravity load rather than the seismic weight and so under-estimated second order effects for single wall models. Check analyses showed that although this was important for displacements near the wall stability limit there was less than 3% difference in displacements on average for wall deformations of up to 3.75% drift, the NZS1170 near fault drift limit. This is deemed insignificant and does not alter the conclusions for these walls.

3.3 Lateral Load Capacity

The validity of the finite element analysis was checked by ensuring that it produced similar load-displacement behaviour as the mechanics based formulation described earlier. For this purpose, a three storey high model building on medium clay was analysed. The predicted lateral force resistance versus the top of wall displacement is shown in Figure 9.

The model building had three floors, and the 3.600 m storey height provides a total height of 10.800 m. Each floor has a seismic weight of 2,000 kN. Lateral load resistance is provided by two walls in each direction, each 3.433 m long (the distance between outer springs for a 3.600 m wall). Each wall supports a gravity load of 500 kN per floor, or 1,500 kN total.

Considering the moment about the centre of the wall, the gravity load creates a self centring moment of 1500 x 3.433 / 2 = 2,574 kN-m and a lateral load at roof level to overcome this or to initiate rocking is 2574 / 10.800 = 238 kN.

For a top of wall displacement, Δ, the seismic weight of the floors creates an additional P-Δ moment which can be calculated by assuming a linear displacement profile, namely,

$$M_{P-\Delta} = 2000\ (\frac{\Delta}{3} + \frac{2\Delta}{3} + \Delta) = 4000\ \Delta$$

This moment is resisted by the two walls in the direction of the lateral load and so the displacement at which the P-Δ moment equals the resisting moment is

$$\Delta = \frac{2574}{4000/2} = 1.287\ m$$

This point corresponds to a displacement in the finite element analysis at which the lateral load capacity is reduced to zero. Figure 9 shows this to occur at a displacement of 1265 mm, which is within 2% of the theoretical value. The difference occurs because the analysis is based on a geometric stiffness formulation which approximates true large displacement effects.

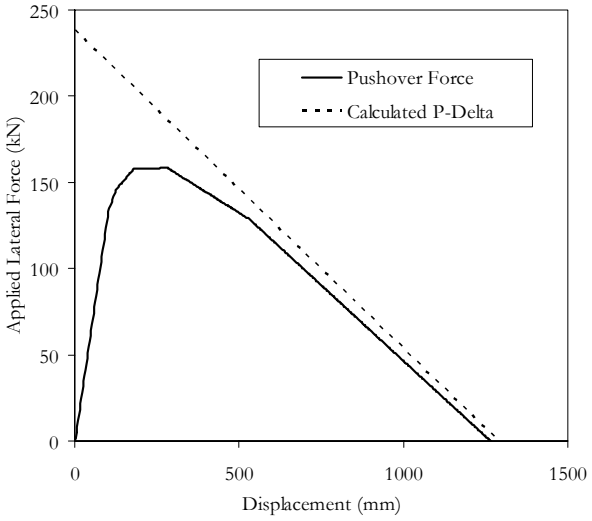

Figure 9. Rocking Block Stability Under Lateral Loads.

The 3.600 m long wall whose response is plotted in Figure 9 will remain stable for a top of wall displacement up to 1.287m, despite the negative incremental stiffness for displacements exceeding 160 mm. If the load lateral load is removed at any displacement less than 1.287 m the wall will return to its original position. If the lateral load is removed at a displacement greater than 1.287 m the wall will continue to tip and complete overturning will occur.

This characteristic of stability against overturning even though the incremental stiffness is negative is termed dynamic stability. A static load implies overturning once the lateral load is sufficient to initiate uplift. However, under dynamic loads a second condition must be satisfied, the displacements must be such that the wall exceeds the stability limit. The nature of the dynamic response to time history loads is such that a wall deformed past the 1.287 m limit may return to the stable region. However, 1.287 m forms a defined and conservative limit for design purposes. Although the stability limit for a rocking block is equal to the width of the block (Figure 2), the limit for a wall structure is usually much less. The wall in Figure 9 reaches its limit at 35% of the wall length. This is because the gravity load on the wall is typically less than the total seismic weight as part of the weight is supported by orthogonal walls or by gravity columns.

Figure 10 plots a portion of the capacity curve for a 3 storey wall. The force versus displacement function is piecewise linear, with a change in slope each time a gap element opens. Initially the positive stiffness provided by more than one gap in compression is greater than the negative P-Δ stiffness but once all but the last gap elements are activated the wall response is purely plastic (defined as no more increase in resistance with increasing displacement). Once this occurs, the net stiffness is negative due to the P-Δ effects. The results from a linear analysis assuming linear soil springs which do not separate under tensile loads are presented in Figure 10 for comparison. This plot shows that the response of the linear system matches that of the rocking wall up to the point where the first gap opens.

The capacity curve plotted in Figure 10 assumes that rocking will occur before any lateral movement at the base of the wall due to sliding. For squat walls with low vertical loads sliding may occur prior to rocking unless the embedment of the base provides sufficient passive pressure resistance to prevent this.

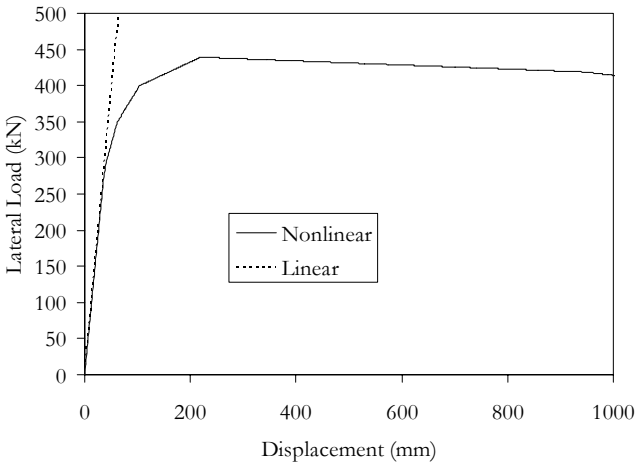

Figure 10. Lateral Capacity of 3 Storey 7.200 m Long Single Wall on Medium Clay Springs.

The loading curve of a rocking wall shown in Figure 10 exhibits similar characteristics to that of yielding structural systems, namely the existence of regions defined by an initial elastic stiffness, strain hardening and reducing strength due to P-Δ effects. However, the response of a rocking wall to cyclic loading, as shown in Figure 11, differs from hysteretic systems. This is because rocking systems are nonlinearly elastic and unloading follows the loading curve, termed elastic unloading. There is no hysteretic area generated and so no hysteretic energy absorption.

For more complex wall configurations the capacity curves exhibit generally similar features to that of single walls but

differ depending on load orientation and the direction of loading.

Figure 12 plots the lateral load capacity curves for a 3 storey U-shaped wall with a 14.400 m long web and 7.200 m long flanges. This wall has an axis of symmetry parallel to the Y axis and so the capacity curves are the same for positive and negative loads along the X axis. In this direction the capacity curve has a positive incremental stiffness up to the maximum displacement of 800 mm plotted because some of the springs along the web remain in contact.

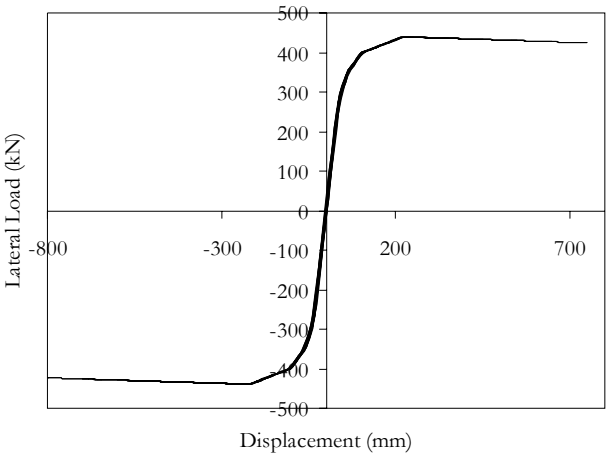

Figure 11. Force-Displacement Response Under Cyclic Loads for 3 storey Wall 7.200 m long on Medium Clay Springs.

For loads in the Y direction the capacity is much lower. This is expected as the wall is only half as long in this direction. The capacity for loads in the positive direction (uplift at the free ends of the flanges) is only one-third that in the negative direction (uplift of the web). The incremental stiffness becomes negative at smaller displacements with loading in the positive direction because only single springs remain in contact.

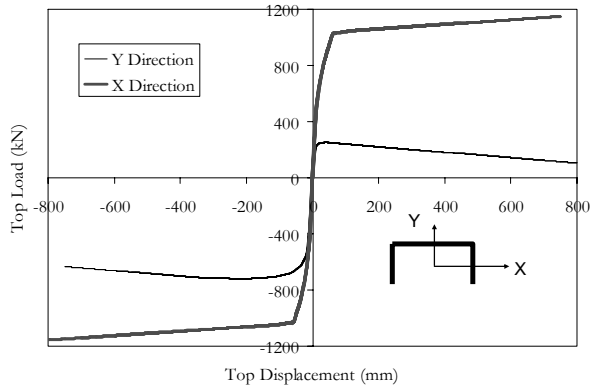

Figure 12. Lateral Capacity of 3 Storey 7.200 m Deep U-Shaped Wall on Medium Clay Soil Springs.

3.4 Input for Dynamic Analysis

NZS1170 specifies that for time history analysis the maximum response from three scaled, recorded time histories be used. US practice permits either this method or, alternatively, the mean response from 7 records. In the latter case, it is common to use records which have been scaled in the frequency domain so as to provide a match to the target spectrum.

For this study, mean results from 7 frequency scaled time histories were used. For each of near fault and far fault locations, and Soil Classes B, C and D, a set of 7 time histories was frequency scaled to match the NZS1170 spectral shape.

The preference for an evaluation procedure based on the mean results from 7 frequency scaled records was selected because this reduced the sensitivity to small changes in period which can result from applying a single scale factor to records. This effect is illustrated by the nonlinear response spectra generated using this procedure. Results for three different yield levels are plotted in Figure 13. Both the acceleration and the displacement spectra varied smoothly as the effective period is increased, in a similar manner to the design spectrum.

The sets of time histories were applied to the prototype walls at 10 scale factors, ranging from ZR = 0.07 to ZR = 0.70 at an increment of 0.07. The maximum factor, ZR = 0.70, is the upper limit of the seismic coefficient specified by NZS1170 for any location in New Zealand and for buildings of any importance factor.

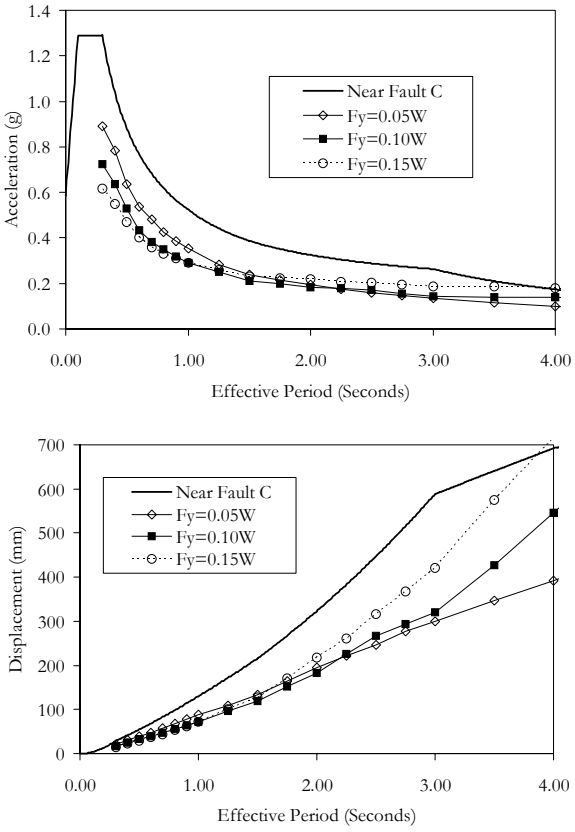

Figure 13. Nonlinear Response Spectra: Mean of 7 Frequency Scaled Records (a) Acceleration Spectra (b) Displacement Spectra.

3.5 Displacements from Nonlinear Analyses

The maximum displacements of the rocking walls were defined as the mean of the peak values from each of the 7 time histories. These varied extremely nonlinearly with amplitude, as shown by the example plotted in Figure 14. These results are for a single storey wall, 3.600 m long, on clay springs. The elastic period for this wall is 0.56 seconds. There are three amplitudes plotted in Figure 15:

1 For a small amplitude earthquake, ZR = 0.07, the displacements were small, 12 mm, and the time between peaks equalled the elastic period, 0.56 seconds.

2 For an increase in amplitude by a factor of 5, to ZR = 0.35, the displacements increased by a factor of 5.7, to 68 mm. The period of the response increased to 0.78 seconds, indicating moderate nonlinearity.

3 Increasing ZR by a further factor of 2 to 0.70 increased the displacement by a factor of 7.4 to 506 mm and the period to 2.19 seconds.

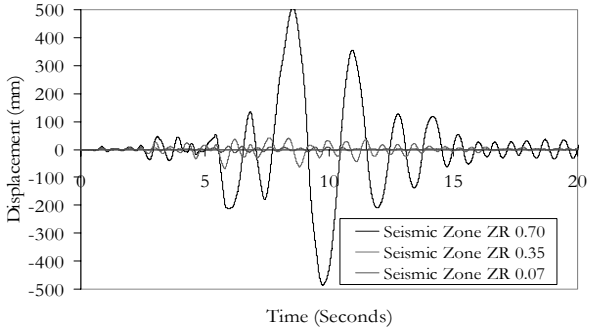

Figure 14. Displacement Time Histories at Top of Wall for Increasing Earthquake Amplitude.

The results indicate an exponential increase in displacements as the earthquake amplitude is increased. This is also evident in Figure 15, where the average displacements are plotted for earthquake amplitudes ranging from ZR = 0.07 to ZR = 0.70 for each of three site classes, both within 2 km of a fault and more than 20 km distance from a fault. For comparison, the expected elastic responses with linear soil springs are also plotted in Figure 15.

Generally, the displacements from the nonlinear analyses show a consistent divergence from the elastic displacements with increasing amplitude of seismic input. For this particular wall, the near fault factor has a relatively minor effect in most cases. There is little difference in the maximum displacements between the near fault and far fault sites for Soil Classes B and C but the near fault displacements reach a maximum about 30% higher than the far fault values for Soil Class D. This is because the effective period of the structure, 0.56 seconds for the elastic case, increases with increasing displacement and for high amplitudes on Soil Class D exceeds 1.50 seconds, the period beyond which the near fault factor influences the response.

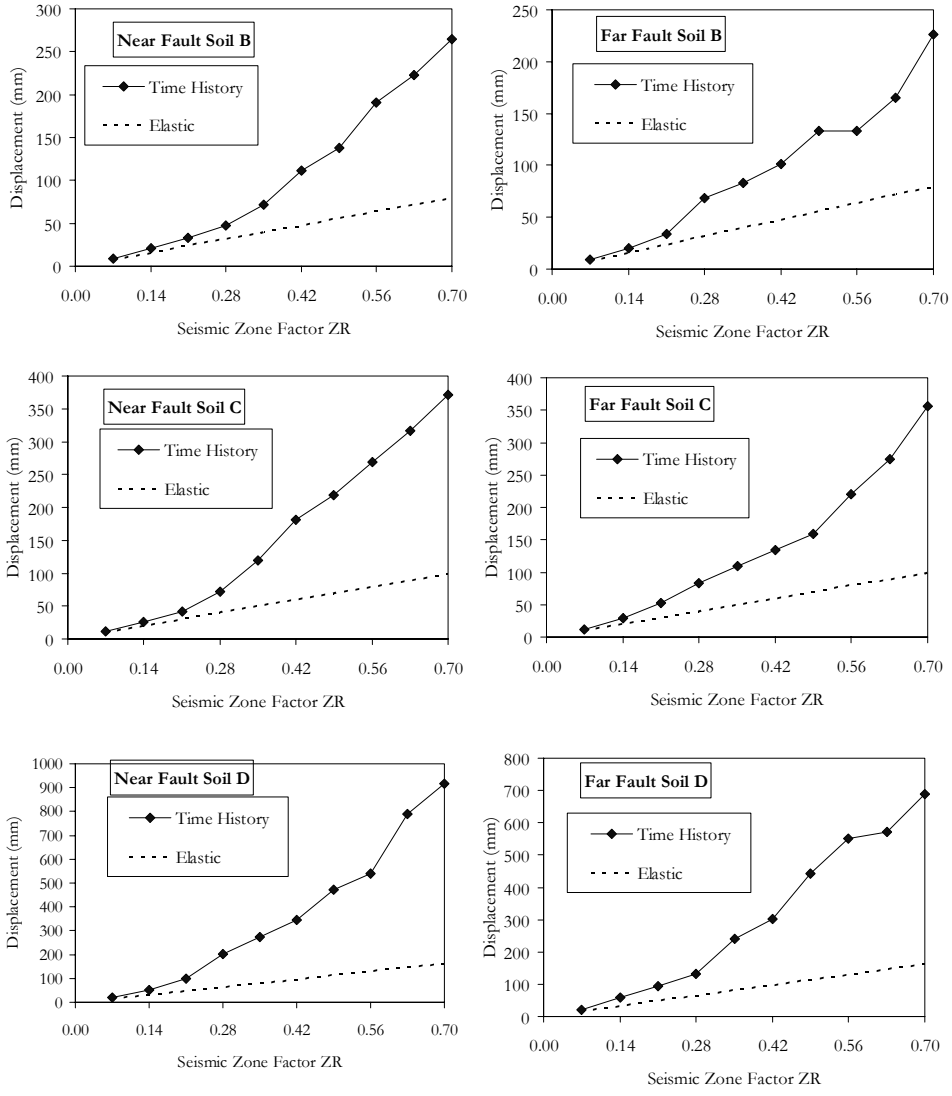

Figure 15. Comparison of Elastic and Nonlinear Displacements Single storey Wall 3.600 m Long on Clay Springs.

3.6 Inertia Force Distribution

The maximum inertia force for a single storey wall can be shown to equal the elasto-plastic strength of the rocking system, within the limits of numerical accuracy of the integration procedure. This equality arises because a single wall model has a single mass.

For multi-storey walls there are multiple masses and each mass may experience a different acceleration and so produce a different inertia force. For equilibrium, the total overturning moment, which is the sum of the inertia forces times the corresponding heights to their centroids, must equal the restoring moment as for single storey walls. However, the base shear force is equal to this moment divided by an effective height which is an unknown quantity.

Figure 16 plots the shear force - displacement data points from the time history analyses of the 3 storey 7.200 m long wall on clay springs and compares them with the static pushover curve. For low amplitude response, where the wall is not rocking, the data points fall on the pushover curve. As the amplitude increases the time history shear force at a given displacement tends to exceed the shear force from the static pushover analysis. The difference increases with increasing amplitude and for very large displacements dynamic forces approach twice the static shear force. The increase of dynamic shear over static shear is termed *dynamic amplification*, and has been recognised in NZ codes for over 20 years, in the requirement for a dynamic amplification factor (ω) to be applied to the seismic shear forces to obtain design shear forces in both ductile frames and ductile shear walls.

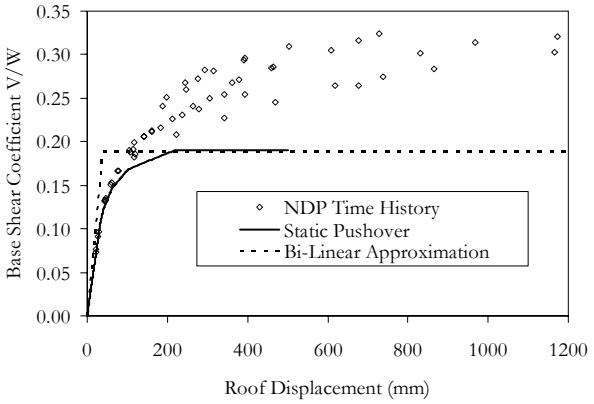

Figure 16. Comparison of Static Capacity Curve with Results from Time History Analysis.

The dynamic amplification effects are illustrated by the time history of response for the three storey model of a 3 storey 3.6 m long wall on medium clay springs, shown in Figure 17(a) and (b) for overturning moment and shear force respectively. For this wall, the net wall length is 3.433 m and the weight 1,530 kN. This provides a theoretical resisting moment of 1530 x 3.433 / 2 = 2,627 kN-mm.

The moment plotted in Figure 17(a) reaches a peak value of 2,047 kN-m, about 20% less than the theoretical limit. The reduction compared to the theoretical limit is because the lever arm is reduced by lateral displacement; therefore the moment capacity reduces during increased rocking as the displacement increases. This provides the characteristic scalloped shape exhibited in Figure 17(a). The maximum time history displacement in this wall is 1686 mm and so the theoretical reduced moment is 1530 x (3.433 – 1.686) / 2 = 1,336 kN-m. It is seen from the plot that this moment occurs at about 28 seconds, which is when the displacement is at the maximum value.

If it is assumed that seismic inertia forces increase linearly with height, as for equivalent static loads, the effective height of application of the inertia forces would be two-thirds the wall height. The maximum moment of 2,047 kN-m would imply a maximum shear force of 2047 / (0.67 x 10.8) = 284 kN.

The concurrent base shear force time history, plotted in Figure 17(b), exhibits much less regularity than the base moment. For both the initial and final portions of the earthquake response the shear force follows a pattern similar to that of the moment. The maximum shear forces in these portions of record are about 250 kN, close to the theoretical value of 284 kN calculated on the assumption that the forces act at two-thirds the height.

In contrast to the start and end portions, the strong motion portion of the record, from about 10 seconds to 30 seconds, exhibits an erratic pattern of shear forces due to an apparent high frequency motion superimposed on the fundamental rocking period of the wall. The shear forces in this strong motion portion of shaking are much higher than in the initial portion, with a peak shear force of 709 kN, 2.5 times the expected shear force of 284 kN.

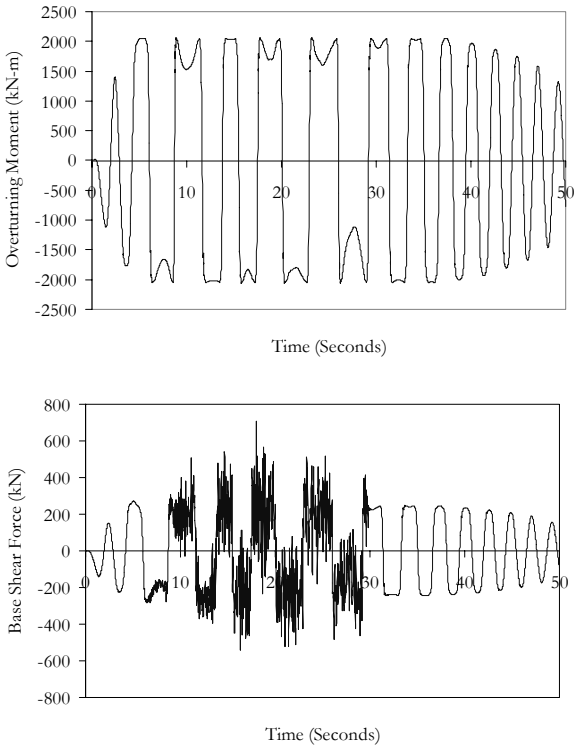

Figure 17. Time History of (a) Rocking Wall Overturning Moment and (b) Base Shear Force.

Capacity design philosophy is based on an assumption that the formation of a ductile mechanism acts as a "fuse" and inhibits increases in forces, other than those due to overstrength and strain hardening. Typically, overstrength and strain hardening add about 50% to the forces at the time of formation of the mechanism for yielding systems. For the wall results reported here, there is no overstrength or strain hardening and so the increase by 150% is due solely to dynamic effects.

The manner in which these effects arise is illustrated by the distribution of inertia forces plotted in Figure 18. The dynamic inertia forces plotted are those occurring at time T = 18.03 seconds, when the base shear force reached a peak value of 709 kN (see Figure 17). It is seen from Figure 18 that the dynamic inertia forces change sign, with a negative force at the top floor and positive force at the lower two floors. The

effect of this is that even though the overturning moment is almost equal to the static overturning moment the shear force is over three times as high. The implies a dynamic amplification factor, ω, of over 3.0

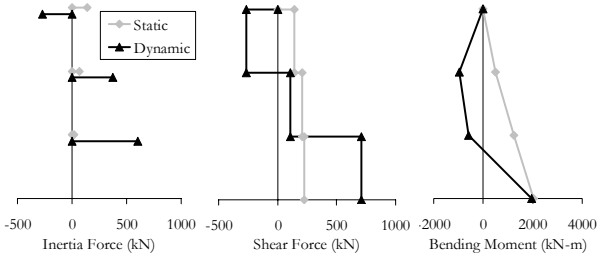

Figure 18. Distributions at Time of Maximum Base Shear.

3.7 Reaction Force

The maximum reaction force on the soil at the base of the single walls is evaluated by tabulating the maximum force in the gap elements at either end of the wall. An example of the variation of this reaction with amplitude is given in Figure 19 for the 3 storey configuration of the 7.200 m long wall.

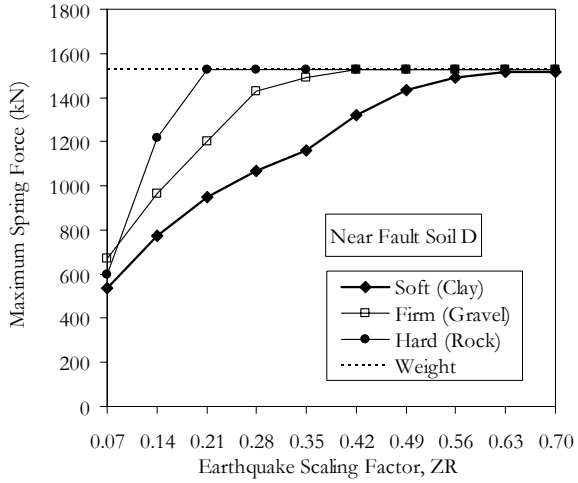

Figure 19. Maximum Reaction Force for Increasing Earthquake Amplitude.

The reaction forces are plotted for all earthquake amplitudes for each of the three soil conditions included in the evaluation. It is noted that,

1 The reaction force increases with increasing earthquake amplitude. This is expected as the wall rocks and the reaction becomes concentrated onto a smaller compression block of soil.

2 The softer the soil springs the slower the increase in reaction force with earthquake amplitude. Again, this is expected because the softer soil springs have a larger gravity load deformation and it takes a larger seismic displacement to disengage the springs.

3 The reaction force converges to the total weight of the wall. At some displacement, all springs except that at the extreme compression end of the wall disengage. At this point, all the weight is supported on a single spring.

The condition where all weight is supported on the end spring is similar to the design office assumption, as illustrated in Figure 3, except that the area of the stress block is based on the spring tributary area rather than calculated from the load eccentricity.

3.8 Impact Effects

The reaction forces described above are the same as would be expected from a static analysis and do not exhibit any dynamic effects, even though some impact force would be expected as the gap elements close. The reason for this is that the analysis model included translational mass only, not vertical mass. This follows normal design office practice for structural analysis.

The effect of ignoring vertical mass on response was assessed by repeating a subset of analyses with a vertical mass corresponding in magnitude to the gravity load on the wall, lumped at the nodes.

Figure 20 shows a portion of the time history of spring deformation and spring force in the extreme gap element for the analyses with and without vertical mass.

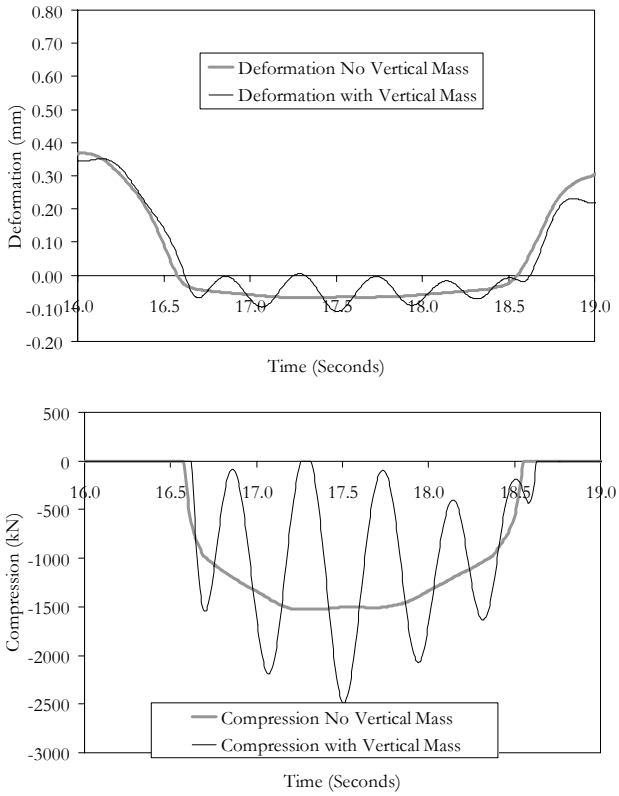

Figure 20. Effect of Vertical Mass on Maximum (a) Spring Deformation and (b)Spring Force.

When vertical mass is ignored, the compression force follows a time history trace approximating the rocking period of the wall, with a period of about 3 seconds between successive peaks during the strong motion portion of record. The amplitude of the peak is limited to the vertical weight of the wall, 1,526 kN. When vertical mass is included in the model there is an additional higher frequency motion superimposed on the long period motion.

For this particular configuration, the period of the high frequency motion is about 0.38 seconds. The displacement trace in Figure 20(a) indicates that when the gap closes the wall "bounces" on the soil spring, causing the compression force to vary by about ±100% from the mean value, where the mean is equal to the value when vertical mass is not included in the model.

The actual behaviour of the soil is more complex than shown in Figure 20 because soil structure interaction includes other important effects, in particular soil nonlinearity (the strain dependence of properties and local soil yielding) and radiation damping. These effects would tend to inhibit the resonance

phenomenon shown in Figure 20 and so the maximum amplification of reaction forces is likely to be much less than that obtained by including full vertical mass.

4. PREDICTING DISPLACEMENTS OF ROCKING WALLS

The 40 single wall configurations, each evaluated for 10 earthquake amplitudes for three soil site classes and two near fault conditions, provided a total of almost 2,400 data points to assess the displacement prediction procedures. For some of the analyses, displacements were large enough to cause collapse and the results were discarded.

FEMA 356 provides three methods to predict displacements in nonlinear systems. One is based on a rocking wall formulation and the other two are variations of the FEMA Nonlinear Static Procedure, the initial effective stiffness and the secant stiffness methods respectively, the latter being based on an ATC formulation [22]. For new buildings, equal displacement and equal energy theories are used to predict displacements of yielding systems.

Variations of the effective stiffness and secant stiffness methods were assessed in an attempt to match the time history response. It became apparent that the secant stiffness method was inappropriate because of the lack of a hysteresis loop area in rocking structures and so this method was abandoned and the development focussed on the effective stiffness method.

Eventually, a variation of the effective stiffness method was developed where the response was based on an effective period but hysteretic damping was ignored. This method provided an excellent correlation with the analysis results.

4.1 Solution Procedure

The displacements are calculated by solving for an effective period, T_e, such that

$$T_e = T_i R_e \quad (1)$$

Where R_e is the response reduction factor defined as:

$$R_e = \frac{C_m C(T_e)}{C_y} \quad (2)$$

Equation 1 is recursive as R_e is a function of the effective period T_e which is the unknown variable. In Equation 2 C_m is the effective mass in the fundamental mode (1.0 for single storey walls), C_y is the force coefficient to initiate rocking and $C(T_e)$ is the NZS1170 design coefficient. In the derivation of $C(T_e)$, it is recommended that the spectral shape factor $C_h(T_e)$ for the response spectrum and time history methods be used as the aim of the procedure is to match time history results.

Once T_e has been calculated from Equation 1, the displacement, Δ, can be calculated from the spectral acceleration using the relationship between spectral acceleration and displacement:

$$\Delta = C(T_e) g \frac{T_e^2}{4\pi^2} \quad (3)$$

It is shown in [8] that in the constant velocity portion of a response spectrum

$$R_e = \sqrt{R_i} \quad (4)$$

From which Equation 1 can be expressed alternatively as

$$T_e = T_i \sqrt{R_i} \quad (5)$$

Equation 5 is not recursive but it is limited to structures where both the initial and effective periods are on the constant velocity portion of the design spectrum.

4.2 Comparison with Analysis Results

The solution procedure was used to compare predicted displacements for 2,390 single wall data points (Figure 21) and 356 multiple wall data points (Figure 22), representing all completed sets of time history analyses. Results are summarized in Table 3.

Table 3. Statistics of the Ratio of Predicted Displacements to Displacements from Nonlinear Analyses.

	Single Walls	Multiple Walls
Number of Data Points	2390	356
Average Ratio	0.94	0.98
Maximum Ratio	2.32	5.03
Minimum Ratio	0.23	0.19
Standard Deviation	0.17	0.56
Slope of Best Fit Equation	0.9812	1.0557

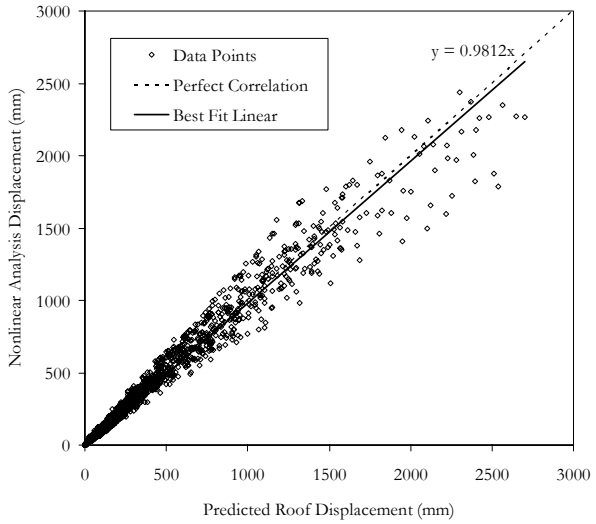

Figure 21. Comparison of Predicted Displacements with time History Displacements for all Planar Wall Models.

1 For the single wall displacements, shown in Figure 21, the slope of the best-fit line equation was 0.9812, very close to the value of 1.0 which would indicate a perfect correlation. As listed in Table 3, the average ratio was 0.94 and the standard deviation of 0.17 indicates a relatively small scatter.

2 For the multiple wall displacements, shown in Figure 22, the slope of the best-fit line equation was 1.0557, again very close to the value of 1.0 which would indicate perfect correlation although not as close as for the single walls. The average ratio was 0.98, very close to 1.0, but for these walls the standard deviation was larger at 0.56, which indicates more scatter in results.

The analysis results plotted in Figures 21 and 22 encompassed a very wide range, more than three orders of magnitude of wall displacements. The simulations covered roof displacements ranging from 0.02 mm to 2,699 mm and 0.8 mm to 371 mm for single walls and multiple walls

respectively. The close correlation for the single walls is extremely good considering this range of applicability.

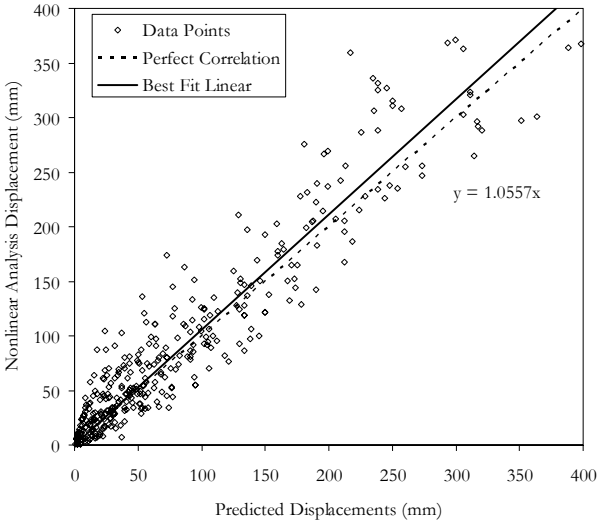

Figure 22. Comparison of Predicted Displacements with time History Displacements for all Non-Planar Wall Models.

4.3 Comparison for Specific Wall Configurations

Results for specific walls are plotted in Figures 23 and 24 for examples of the single and multiple wall models respectively.

Figure 23 compares the displacements from the time history analysis for a single storey 3.600 m long single wall model with those predicted by the equations above for three different soil classes for both near fault and far fault conditions. The predicted displacements provide a good match to the results from the time history analyses for all site conditions and earthquake amplitudes. The calculated displacement function tends to form a smoother profile than the analysis results for increasing amplitude, which is to be expected as the former are based on calculations from smoothed design spectra and the latter on mean results from 7 time histories.

Figure 24 provides a similar comparison of predicted to analysis displacements, in this case for a 3 storey, 7.200 m x 14.400 m U-shaped wall. Results are calculated for the three soil classes and all are based on the near fault spectral shape. Results are plotted for both the X and Y directions as this wall is not symmetrical (see Figure 12 for the capacity curve and axis orientation for this wall). For X direction loads the wall is loaded about an axis of symmetry and has equal strength properties for both positive and negative direction loads. In this direction, the design procedure accurately predicts the analysis displacement.

For Y direction loads the wall response is not symmetrical and Figure 24 shows that the predictions are much less accurate in this direction, especially for displacements exceeding about 100 mm. The strength of the wall differs for the positive and negative directions of load and it was found that the design procedure produced a better correlation when the lower of the two strengths was used to define C_y.

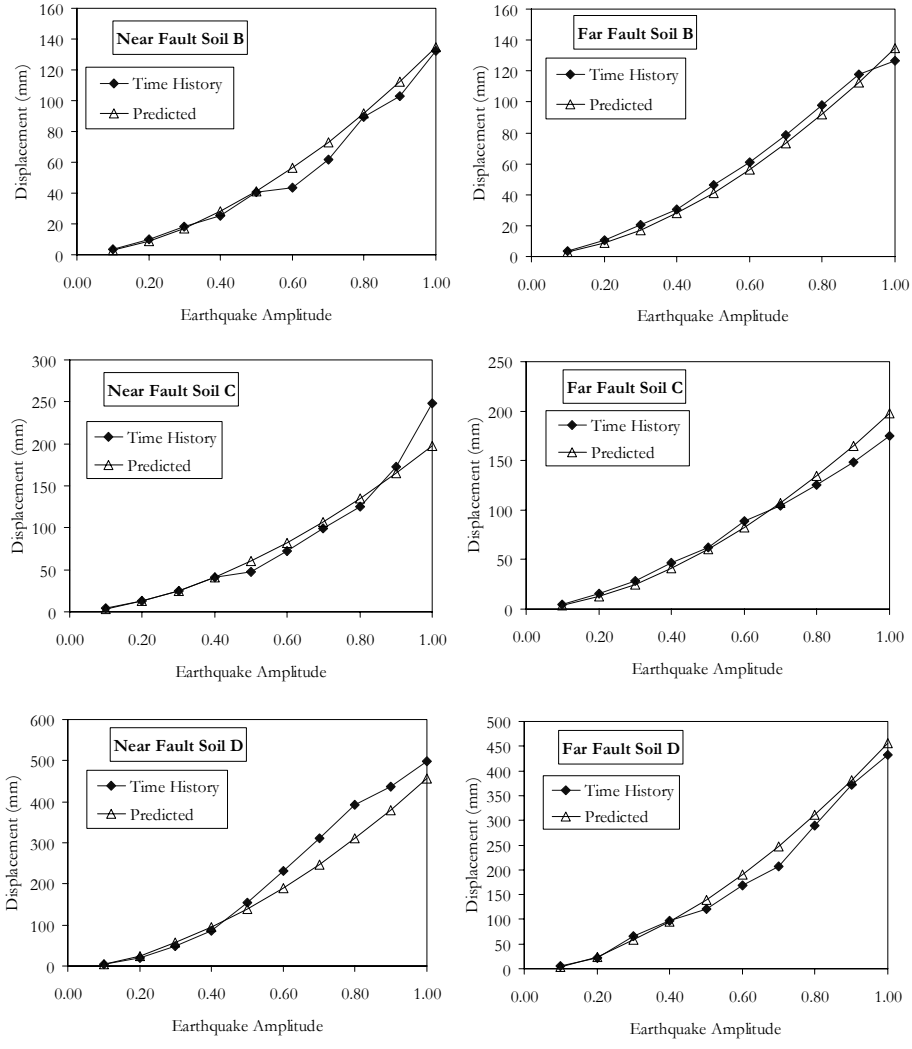

Figure 23. Displacements in 3.600 m Long Single Storey Wall on Medium Gravel.

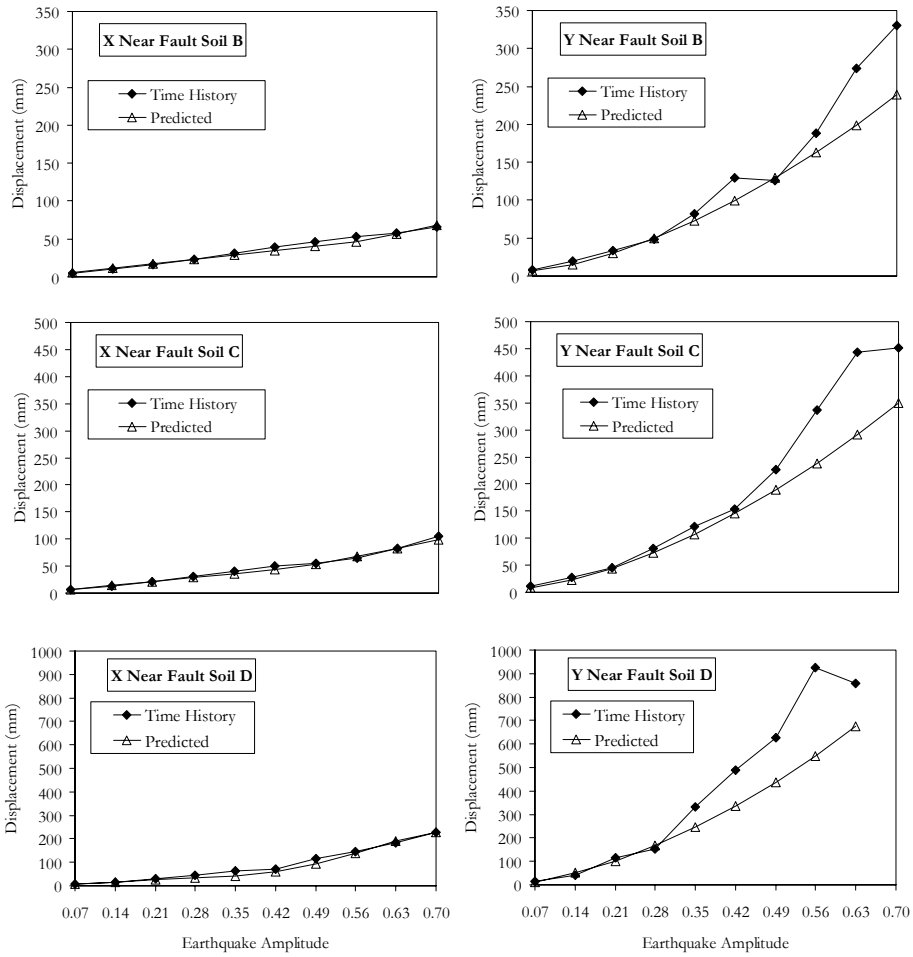

Figure 24. Displacements in U-Shaped Wall 7.200 m x 14.400 m, 3 Storey Medium Clay.

4.4 Torsional Increases in Displacements

The number of three dimensional structures evaluated was insufficient to fully develop procedures to estimate increases in displacement due to torsion. The limited studies suggest that the calculated displacement be increased by the higher of two factors:

1 A factor equal to two times the calculated actual eccentricity. For example, if the calculated eccentricity is 0.20B, allow for a 40% increase in displacements.

2 A factor equal to the accidental eccentricity. For design to NZS 1170, this requires a minimum 10% increase in displacements due to 0.10B eccentricity.

Figure 25 plots the data points for each analysis of the three dimensional models for which the maximum drift was less than the NZS 1170 limit of 3.73%. This limit applied as all analyses were for near fault conditions and a 0.67 reduction factor applies. Also plotted for each model is the increase resulting from the higher of the two factors calculated as above.

The torsional increase in displacements for each of the analyses which provided the data points in Figure 25 are calculated as $(\Delta_{MAX}- \Delta_{CM})/\Delta_{CM}$ where Δ_{CM} is the centre of mass displacement and Δ_{MAX} is the maximum displacement anywhere on a floor, typically at one corner. Both displacements are parallel to the same horizontal axis.

For each of the three models there were 180 analyses with the floor centroid at the calculated centre of mass plus 60 analyses with the centroid moved by either a positive or negative eccentricity equal to 0.10 times the floor dimension. This provided 240 possible data points for each wall.

All walls show a clear pattern that the increase in displacements due to torsion reduces as drifts increase, although this is less marked for the 14.400 x 14.400 m U-shaped wall than for the other two walls. Because of this, the recommended increase is conservative beyond a particular drift limit which depends on the wall configuration:

1 For drifts exceeding 1.15% for the 14.400 m x 14.400 m U-shaped wall.

2 For drifts exceeding 0.29% for the 7.200 m x 14.400 m U-shaped wall.

3 For drifts exceeding 0.14% for the model with 3.600 m and 7.200 m walls.

For design, this trend is fortuitous in that it ensures that the calculated displacements will be conservative when drifts are large and deformations are likely to be critical. When the formula is non-conservative the numerical values are likely to be small anyway and so the under-estimate of displacements will have less effect.

5. DYNAMIC AMPLIFICATION OF SHEAR FORCES

The dynamic inertia force distribution for multi-story walls varies from the static distribution, resulting in an increase in maximum shear force over what would be expected from a

static analysis. This effect is not unique to rocking walls and is the reason NZS3101 [23] defines a dynamic shear magnification factor for ductile shear walls.

Amplification factors were derived from results in which the peak drift was within the NZS 1170 limits (2.50% for motions without near fault effects and 2.50/0.67 = 3.73% for near fault motions).

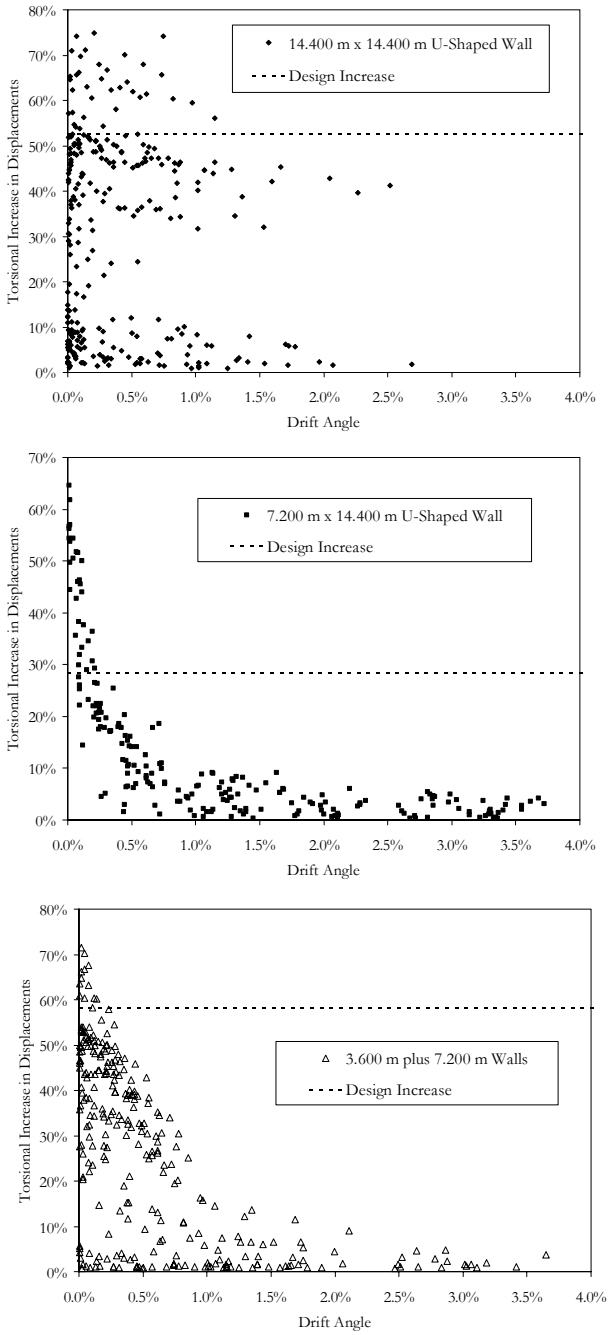

Figure 25. Torsional Increases in Displacement for Three Dimensional Wall Models.

Figure 26 plots the maximum shear force amplification factor for each wall greater than one storey high, where the amplification factor is defined as the maximum base shear force from the nonlinear analysis divided by the shear force calculated to initiate rocking. This shows that an equation defining amplification as a function of the number of stories, similar to that specified by NZS3101 for ductile walls, requires much higher amplification factors for rocking walls if it is to envelope all recorded values.

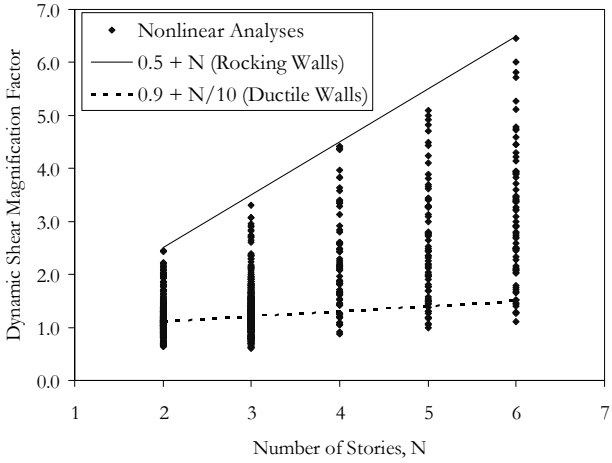

Figure 26. Dynamic Amplification of Shear Forces for all Multi-storey Single Wall Models.

An examination of the detailed results showed that there were definite trends for the amplification factors:

1 The amplification factor strongly correlates to the number of stories, and increases with increasing number of stories for all walls and all soil spring stiffness values.

2 The amplification factor is relatively insensitive to the length of the wall for a specified number of stories.

3 The amplification factor is strongly correlated to the ductility demand. This agrees with conclusions from other studies which have indicated that the stronger the degree of nonlinearity the more pronounced the dynamic amplification effects [24].

4 The amplification factor increased with increasing soil spring stiffness but by a much smaller factor than the increase due to an increasing number of stories.

Based on the results from the time history analyses, a formulation for the shear amplification factor was developed based on a coefficient, as listed in Table 4, applied to the ductility factor (DF) with the equation in Figure 27 forming an upper limit:

$$\omega_V = 1 + a_{VN}DF \leq 0.5 + N \qquad \text{for } N > 1 \tag{6}$$

Table 4. Shear Amplification Factor.

N	Amplification Factor
Number of Stories	a_{vn}
1	0.00
2	0.10
3	0.15
4	0.40
5	0.60
6	0.90

If the shear amplification is a function of the extent of rocking of the wall then it would be expected that the value would be unity for ductility factors up to 1, where rocking does not occur. This would imply that Equation 6 would be of the form $1 + a_{VN}$ (DF-1). However amplification factors were greater than 1 for walls designed for DF = 1, especially for the taller walls. The reason for this is that the elastic shear distribution in the walls does not correspond to a uniform distribution due

to higher mode effects, which are more pronounced for taller walls.

Figure 27 compares the amplification factors calculated from Equation 6 with the data points extracted from the single wall models. The upper limit governed only the 5 and 6 storey variations. The shear amplification factors will be conservative for some configurations, especially for the high structures with high ductility factors.

Figure 28 compares the shear amplification factors with the analysis results for each of the three multiple wall models. Generally, the formula provides a reasonable, and conservative, estimate of actual shear amplification. The formula appears to be more conservative for the 7.2 m U-Shaped wall and the non-symmetrical wall than the 14.4 m U-Shaped wall.

The amplification factors are applied to the wall yield force. In most walls the amplified rocking shear force will be less than the elastic shear force in a similar wall which is fixed against rocking and responding elastically. For example, if a 3 storey wall has a ductility factor of 4 the design shear force will be the yield force times (1 + 4 x 0.15) = $1.60F_y$. However, by definition the elastic (non-rocking) force will be the ductility factor times the yield force = $4F_y$. Therefore, the rocking shear force will be 1.60 F_y / 4 F_y = 40% of the shear force which would occur in the wall if rocking were restrained. This illustrates how rocking reduces seismic forces, even when dynamic effects are incorporated.

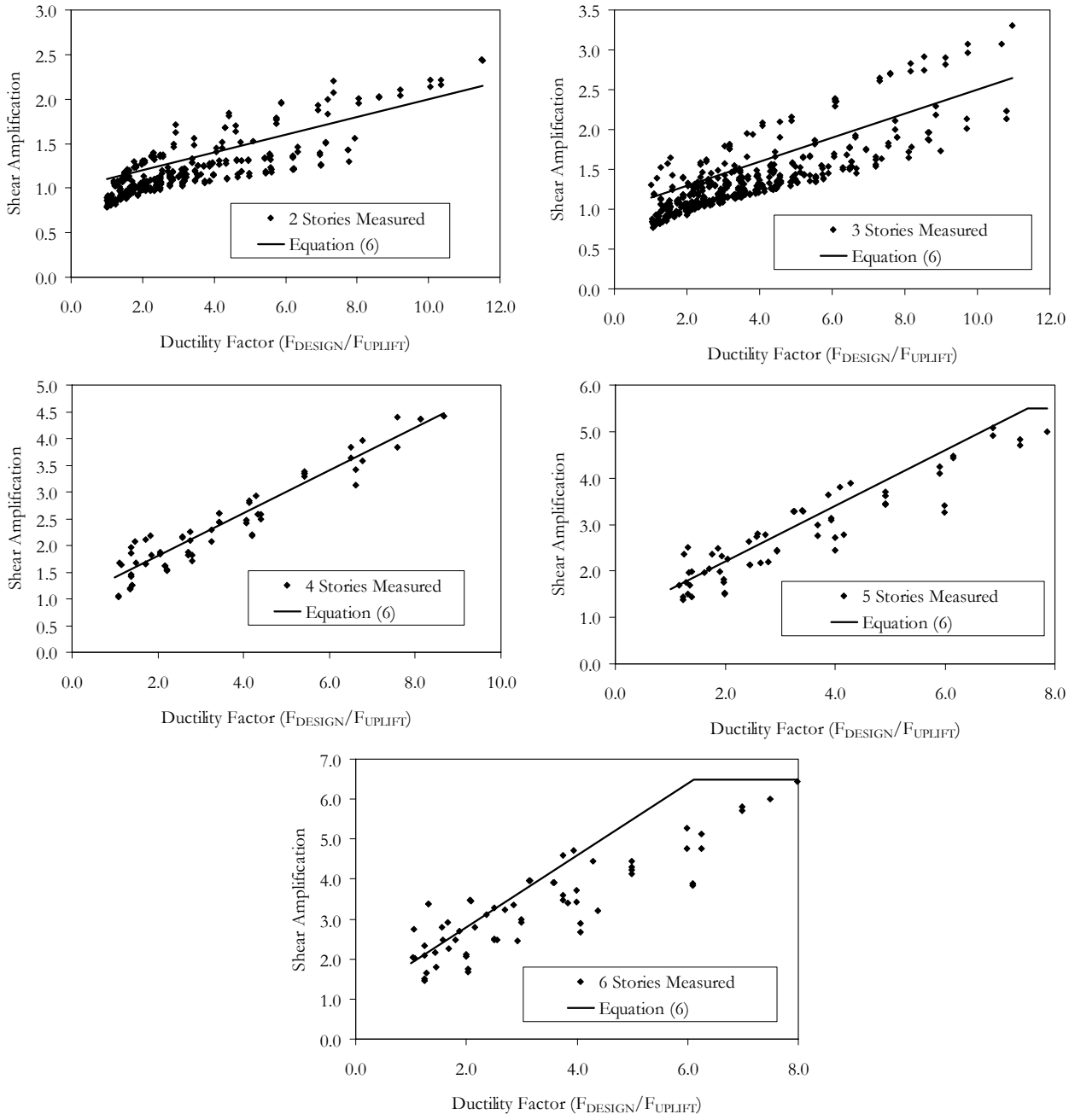

Figure 27. Shear Amplification for all Single Wall Models.

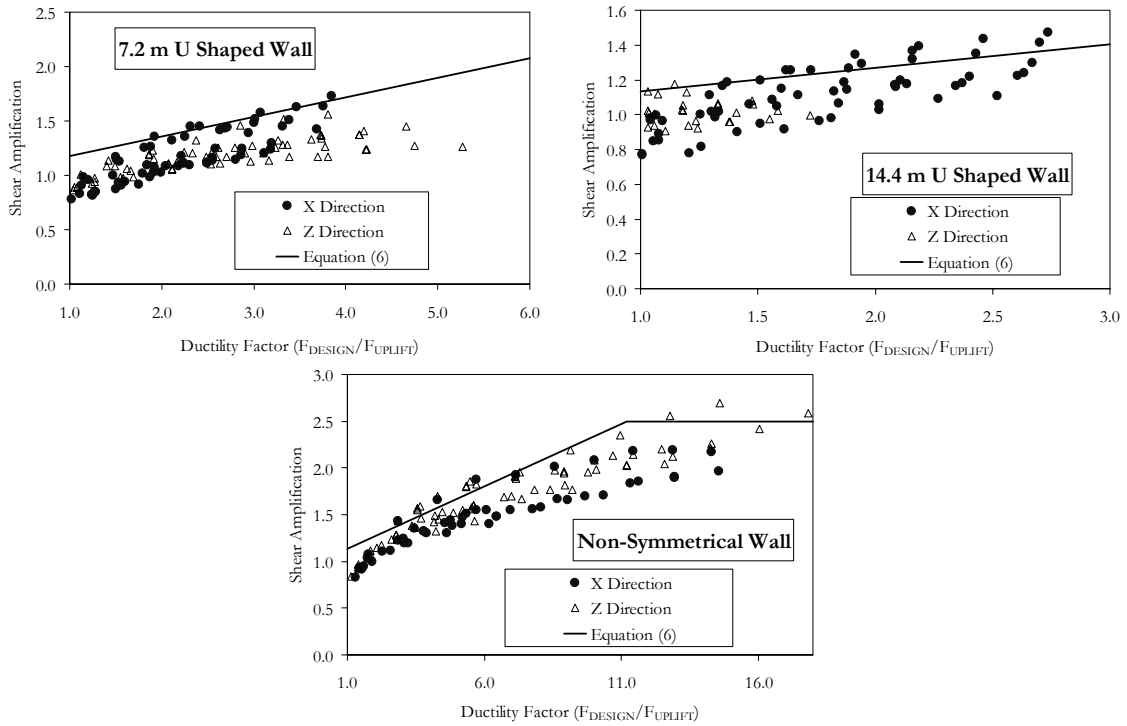

Figure 28. Shear Amplification for all Multiple Wall Models.

6. COMPARISON OF ROCKING AND YIELDING RESPONSE

To assess the differences in response between systems characterised by rocking and by material yielding, two of the single wall examples were re-evaluated with fixity at ground level and nonlinearity due to plastic hinging at the base rather than by rocking. The seismic response of these two systems was compared with the response of an equivalent elastic system, which was a wall on elastic soil springs with no uplift or material nonlinearity. The comparison was performed for two examples, one a relatively squat wall and the second a slender wall.

6.1 Three Storey 7.200 m Long Wall

The three storey configuration of the 7.200 m long wall on rock springs was modified to a fixed base model. This wall was a relatively squat configuration, with a height to width ratio of 1.5:1. Strength properties were based on a steel reinforcing ratio of 0.25% throughout and material nonlinearity was due to both shear cracking and flexural yielding. This procedure has been shown to be capable of predicting displacements accurately in a full scale test of a yielding wall [24].

The wall hysteresis curve, as shown in Figure 29, was generated by applying a cyclic displacement to the top of the model. The cyclic response shows a "pinched" hysteresis loop, typical of axially loaded reinforced concrete elements.

Figure 31 compares the maximum displacements at the top of the wall for the yielding model with the equivalent displacements obtained from the rocking model (plots on left hand side). Also included on Figure 31 are displacements for the elastic wall. General trends shown by this plot are:

1 Yielding walls produced displacements on average 3.3 times higher than the elastic response.

2 Rocking walls produced displacements on average 5.4 times higher than the elastic response.

3 The rocking mode of response produced displacements higher than the yielding response by an average of approximately 60%.

Generally the proportional differences between the different systems were relatively small for low seismic amplitudes and increased within increasing amplitude. This is presumably because of the lower energy dissipation and the lower "post-yielding" stiffness of the rocking wall compared to the yielding wall. These effects would become relatively more important as the seismic input increased.

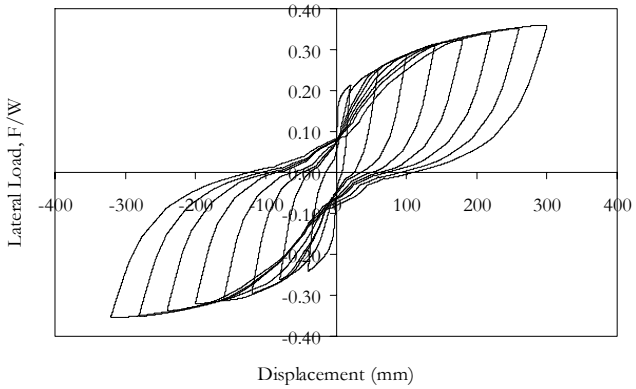

Figure 29. Hysteresis for 3 Storey High 7.200 m long Yielding Wall.

6.2 Five Storey 3.600 m Long Wall

The model of the five storey configuration of the 3.600 m long wall on rock springs was also modified to a fixed base model. This was a slender configuration compared with the previous wall, with a height to width ratio of 5:1. Strength properties were based on a steel reinforcing ratio of 1.0% throughout and

material nonlinearity was due to both shear cracking and flexural yielding. The wall hysteresis curve, as shown in Figure 30, again shows a "pinched" hysteresis loop typical of axially loaded reinforced concrete elements.

The plots on the right hand side of Figure 31 compare the displacement for the three configurations of the 5 storey wall. General trends shown by this plot are:

1 Yielding produced displacements on average 1.66 times higher than the elastic response.

2 Rocking produced displacements on average 2.18 times higher than the elastic response.

3 The rocking mode of response produced displacements higher than the yielding response by an average of approximately 30%.

The relative order of the displacements is the same for this slender wall as for the squat wall but the differences between the three configurations is generally proportionally smaller.

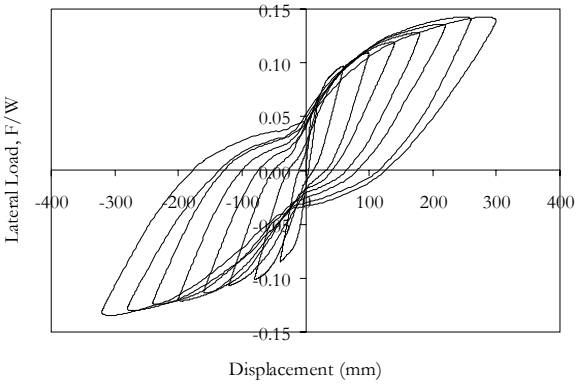

Figure 30. Hysteresis for 3 Storey High 7.200 m long Yielding Wall.

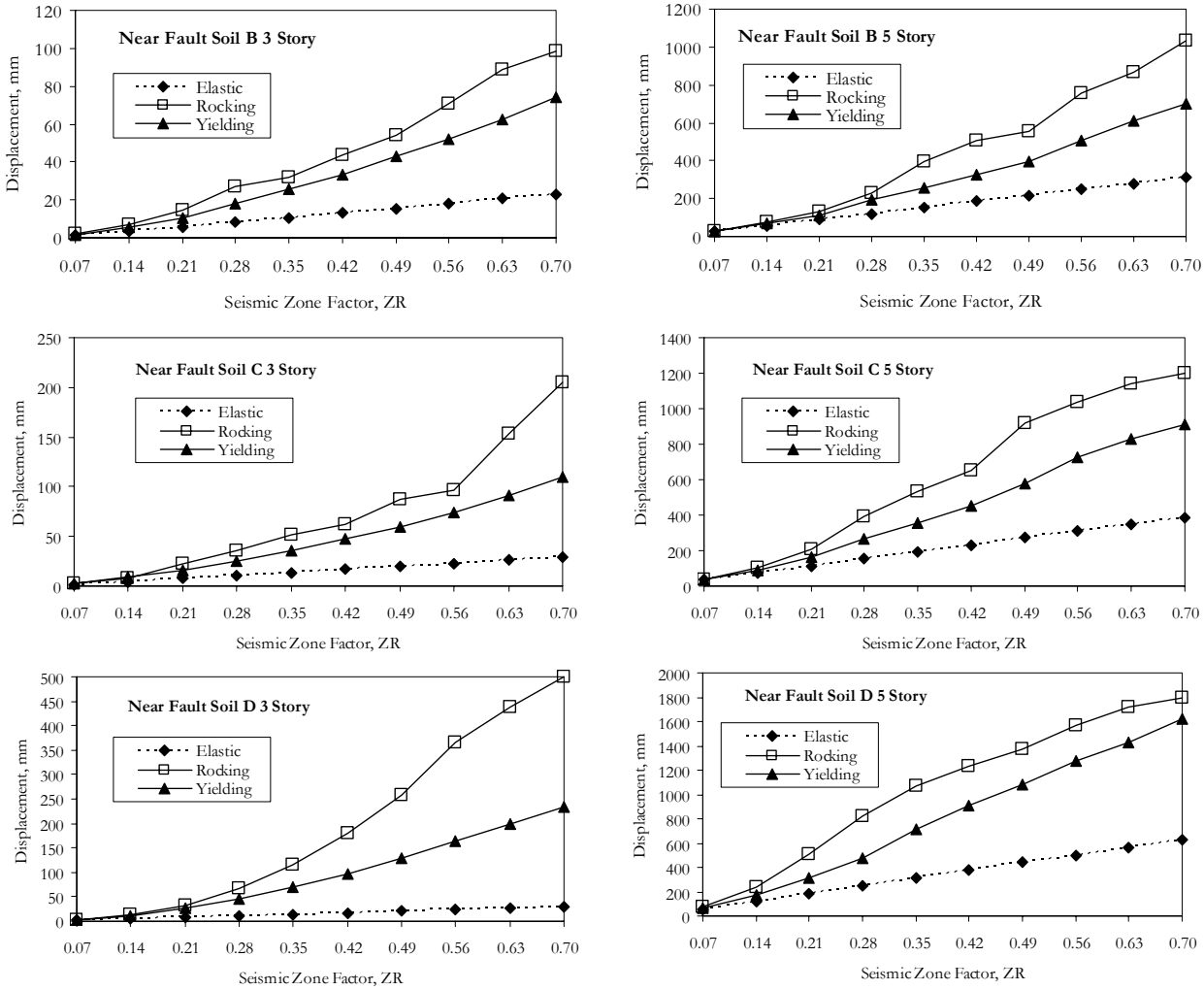

Figure 31. Comparison of Yielding and Rocking Displacements for 3 Storey Wall.

6.3 Comparison of Response

Table 5 compares the peak response for the elastic, yielding and rocking walls, for moderate (ZR= 0.28) and very high (ZR= 0.70) seismic loads. The shear amplification is defined here as the ratio of maximum base shear from the time history analysis to (a) the spectral acceleration times the seismic mass for elastic walls or (b) the strength from the capacity curve at the seismic displacement for yielding walls or (c) the rocking strength for rocking walls. The shear amplification may be less than unity for the elastic wall because the mass participation is less than 100%.

Three major findings from the analyses are:

1 The displacements from a yielding wall are always higher than that from an elastic wall and always lower than that from a rocking wall. The differences are more pronounced for squat walls than slender walls and for high seismic zones than low seismic zones.

2 The maximum base shear is generally similar for the rocking and yielding walls. In both cases, the maximum base shear is much lower than that found for the elastic wall.

3 The rocking walls have greater shear amplification factors than the yielding walls. For both rocking and yielding walls the shear amplification is higher for the 5 storey wall than for the 3 storey wall and is higher in the high seismic zone than in the low seismic zone.

Table 5. Comparison of Peak Response Quantities.

Zone	Condition	Δ	$\frac{V_u}{W}$	Shear Amplification, ω
3 storey squat wall				
ZR=0.28	Elastic	11	0.76	0.90
	Yielding	48	0.31	1.00
	Rocking	90	0.36	1.89
ZR=0.70	Elastic	31	1.94	0.92
	Yielding	192	0.55	1.32
	Rocking	383	0.54	2.84
5 storey slender wall				
ZR=0.28	Elastic	245	0.48	0.91
	Yielding	374	0.20	1.72
	Rocking	531	0.25	3.78
ZR=0.70	Elastic	615	1.24	0.94
	Yielding	1068	0.42	3.44
	Rocking	1416	0.44	6.67

7. TENTATIVE SEISMIC DESIGN PROCEDURE

7.1 Applicability

These design procedures are intended for shear wall structures which rock under seismic loads. As the development was based on the results of an extensive series of analysis on single walls and a more limited evaluation of multiple wall buildings and non-symmetrical buildings, the accuracy of the procedures will be best for:

1. Low rise walls, three stories or less.
2. Regular, symmetrical shear wall buildings.
3. Walls with relatively small ductility factors (DF), with a rocking strength (static restoring moment) of one-quarter or more of the elastic demand (DF less than 4).

The designer selects a foundation size either to meet serviceability requirements or to provide a rocking strength corresponding to a selected ductility factor. The performance is then assessed and the foundation size adjusted as required to achieve the design objectives.

7.2 Notation

a_{VN} Coefficient for dynamic amplification factor
B Foundation width
$C(T_e)$ NZS1170 elastic coefficient at effective period.
$C_d(T_1)$ NZS1170 design coefficient at initial period.
C_0 Coefficient relating spectral displacement to roof displacement.
C_m Effective mass factor.
C_y Yield coefficient for rocking wall
c Length of compressive stress block at toe of wall
D Building dimension at right angles to direction of rocking (plan dimension to define eccentricity)
DF Ductility factor
F_y Applied lateral load at rocking
G Soil shear modulus
g Acceleration due to gravity
H Wall height
H_i Height to the i th floor
k_i Stiffness of soil spring i
K_R Rocking stiffness
L Wall length
M Total seismic mass tributary to wall
m_i Seismic mass of i th floor
M_R Rocking mass moment of inertia
N Number of stories
q_c Ultimate soil strength
R_e Response reduction factor at effective period
T_e Effective period of rocking wall
T_1 Initial period of rocking wall
T_R Rocking period
T_W Period of fixed base wall
V_e Elastic base shear on wall from NZS1170
V_u Ultimate seismic shear force on wall
W Weight on wall
x_i In-plane horizontal distance to soil spring i from centroid of wall
y_i Out-of-plane distance of element i from the baseline of eccentricity calculation
υ Poisson's ratio of soil
ω_v Dynamic amplification factor for wall shear

7.3 Soil Properties

Soil properties will usually be obtained from soils reports for particular projects. Where project specific values are not available, approximate values can be selected from Table 6 but in this case the sensitivity of response to changes in the values should be assessed.

Table 6. Range of Soil Properties.

Soil	Shear Modulus G (kPa)	Poisson's Ratio ν	Failure Stress (kPa)	ULS Stress (kPa)
Rock	800,000	0.25	4000+	2000+
Dense Gravel	80,000	0.30	1000	500
Medium Gravel	to	to	400	200
Dense Sand	40,000	0.40	600	300
Medium Sand			300	150
Stiff Clay	20,000 -	0.5	300	150
Medium Clay	2000		150	75

A soils report provides the ultimate, or failure, strength as defined by the geotechnical consultant. For structural design

the Ultimate Limit State (ULS) strength, defined as q_c in these procedures, is generally taken as one-half the failure stress. The reduced ULS value results in a larger compressive block than if the failure strength were used, and consequently the rocking strength is lower than was used for the analysis models. The FEMA spring model depicted in Figure 1 tends to correlate to the failure strength rather than the ULS value. Pending further research, it appears that the best approach may be to use the ULS value to develop minimum foundation size but to use the failure strength to assess performance.

7.4 Step-by-Step Procedure

Step 1: Define the Foundation Size

For elastic (non-rocking) response, the required foundation width can be calculated from the applied elastic seismic load, $V_e = C_d(T_1)$ Mg, the wall length at foundation level, L, and the soil ultimate bearing capacity, q_c, as

$$B = \frac{W}{q_c(L - \frac{2V_eH}{WC_O})} \tag{7}$$

(See Step 5 below for a definition of C_o).

For a rocking wall, the foundation length and/or width will be set at some value smaller than that defined above and the performance will be checked at the DF resulting from the rocking wall, following the steps listed below.

The absolute minimum foundation width is

$$B > \frac{W}{q_c L} \tag{8}$$

The starting trial foundation width must be larger than that specified by Equation 8. To calculate the width for a specific DF, replace V_e with V_e / DF in Equation 7. This permits the relationship between foundation size and ductility factor to be assessed. Figure 32 illustrates this relationship for a sample 3 storey wall. It can be seen that the ductility factor can be reduced by increasing the foundation width or by extending the foundation beyond the wall, increasing L.

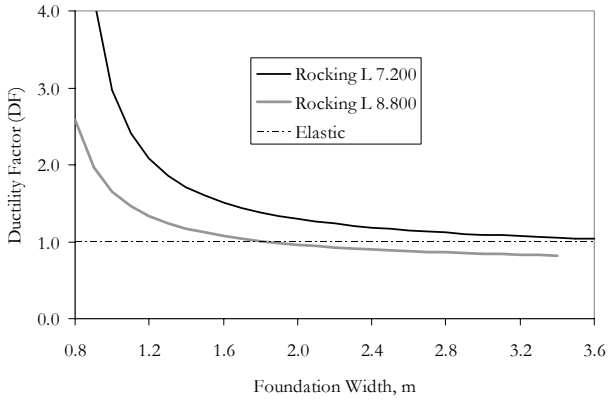

Figure 32. Foundation Size for 3 storey Wall 7.200 m Long with q_c = 300 kPa for Z = 0.20.

If the foundation width, B, exceeds the width specified in Equation 7 the wall will not rock and the procedures for rocking displacement and dynamic amplification are not required. A limit on the base shear can be derived from Equation 7, beyond which the wall will rock regardless of foundation width, as:

$$V_e > \frac{LWC_0}{2H} \tag{9}$$

Step 2: Calculate Soil Spring Stiffness

Foundation stiffness properties can be calculated using the spring definition from FEMA 356 Figure 4-5 (reproduced as Figure 1 in this paper) or other sources. For New Zealand sites, a typical range of soil properties is as listed above in Table 6.

Step 3: Estimate Period

Either extract the period from a linear elastic model of the wall or use the approximate formulas in Section 2.5 of this paper. The soil spring stiffness, required for the period calculations, is that calculated from FEMA 356 procedures in Step 3.

Step 4: Calculate the Compression Block Size

Calculate the length of the compression block as

$$c = \frac{W}{q_c B} \tag{10}$$

Step 5: Calculate Wall Rocking Strength

Calculate the yield force to initiate rocking. For a symmetric wall:

$$F_y = \frac{W(\frac{L}{2} - \frac{c}{2})}{\frac{H}{C_0}} \tag{11}$$

From this, the yield coefficient is calculated as:

$$C_y = \frac{F_y}{Mg} \tag{12}$$

For non-symmetric walls, such as C shaped and L shaped sections, the moment capacity ($W(\frac{L}{2} - \frac{c}{2})$ in Equation 11) can be calculated by taking moments of the reaction forces in individual springs about the wall centroid.

The coefficient C_0 relates spectral displacement to the roof displacement for multi-storey walls. It has a value of 1.0 for single storey buildings and increases with height in a range of between 1.2 and 1.5 for higher buildings. FEMA 356 provides tabulated values.

Step 6: Calculate Seismic Displacements

The single degree of freedom displacement is calculated from the relationship between acceleration and displacement as:

$$\Delta = C(T_e)g\frac{T_e^2}{4\pi^2} \tag{13}$$

The displacement at the top of the wall is calculated as

$$\Delta_{TOP} = \Delta C_0 \tag{14}$$

The effective period is calculated from the elastic period as:

$$T_e = T_1 R_e \tag{15}$$

R_e is the response reduction factor, defined as:

$$R_e = \frac{C_m C(T_e)}{C_y} \tag{16}$$

C_m is the effective mass factor obtained from a modal analysis or, alternatively, tabulated values from FEMA 356 may be used (typically 1.0 for 1 or 2 storey buildings, 0.8 or 0.9 for taller buildings). Note that the equation for effective period is recursive as R_e is a function of T_e which is the unknown variable.

Step 7: Calculate Structural Ductility Factor

Structural ductility factor

$$DF = \frac{C(T_1)}{C_y} \quad (17)$$

Step 8: Assess Dynamic Amplification Effects on Wall Shear

$$V_U = F_Y \omega_V \quad (18)$$

$$\omega_V = 1 + a_{VN} DF \leq 0.5 + N \quad \text{for N > 1 storey} \quad (19a)$$
$$= 1.0 \quad \text{for N = 1 storey} \quad (19b)$$

Values of a_{VN} for different numbers of stories are listed in Table 4.

Step 9: Calculate Torsional Increase in Displacements

From the limited results on three-dimensional models, it is recommended that displacements be increased by a factor which is the higher of:

1 Two times the calculated actual eccentricity. For example, if the calculated eccentricity is 0.15B, allow for a 30% increase in displacements.

2 A factor equal to the accidental eccentricity. That is, allow a 10% increase in displacements for the minimum specified eccentricity of 0.10B in NZS1170.

As discussed previously, the number of analyses including torsional effects was limited. The above recommendations are empirical and there appears to be no theoretical basis for the lesser effect of accidental eccentricity than actual eccentricity. One possible reason for the difference is that accidental eccentricity is applied to the seismic mass but not to the gravity loads and therefore does not modify the location of the centre of resistance in the same manner as the centre of mass.

The effects of torsion need to be the subject of further research, both for this effect and also the apparent amplitude dependence of torsional effects exhibited by the results in Figure 25.

Step 10: Assess Performance

The performance of the wall, as defined by maximum displacements and dynamic amplification effects, is assessed to determine whether it achieves the project design objectives. If not, the foundation size is adjusted and the procedure repeated from Step 2 above. Increasing the foundation size decreases the ductility factor, which reduces both displacements and dynamic amplification effects. However, it will also increase the shear force to initiate rocking so may not result in a net decrease in design shear force.

7.5 Example Applications of Design Procedure

Appendix A of this paper provides four examples of the application of this design procedure, two planar wall configurations and two non–planar wall configurations. Each of these configurations was equivalent to one of the walls selected for the analyses and so time history results were available for comparison.

Table 7 compares the displacements and base shear coefficients for each example, as obtained from the design procedure, and the time history results. Full calculations are provided in Appendix A. For each analysis, the design procedure was implemented for two assumptions of soil strength, firstly equal to the ULS stress (q_c) and secondly with a soil strength equal to the failure strength ($2q_c$). The four examples represented walls of increasing complexity and the comparisons of design procedure predictions with the time history results illustrated that the prediction was better for the simpler models:

1 Example 1 was a single wall. The design procedure displacements prediction matched the analysis results well. The match with the time history base shear was improved when the failure strength ($2q_c$) was used.

2 Example 2 was two planar walls. The match was not as good as Example 1 but still reasonable. Both the displacements and base shear predictions improved when the failure strength ($2q_c$) was used.

3 Example 3 comprised walls of different length on each side of the building. The design procedure overestimated the displacements but not excessively so. Shear forces were under-estimated unless the failure strength was used instead of the ULS.

4 Example 4 comprised a U-shaped wall. For X direction loading, the match was poor when the approximate formulas were used to calculate the period and the values of C_0 and C_m were selected from FEMA tables. The match improved when properties from a modal analysis were used. In the Y direction the wall is symmetrical and the approximate formulas provided a good estimate of displacements but overestimated shear forces.

From these results, it appears that use of the ULS strength provides a good estimate of maximum displacements but tends to under-estimate the base shear coefficient. The base shear coefficient is more conservative if the failure strength is used, although this may slightly under-estimate displacements for some walls.

Table 7. Displacements and Base Shear Predictions from Design Procedure and Results from Time History Analysis.

	Displacements (mm)			Base Shear Coefficient, C		
No.	**Time**	**Procedure**		**Time**	**Procedure**	
	History	**q_C**	**$2q_C$**	**History**	**q_C**	**$2q_C$**
1	47	49	43	0.23	0.18	0.21
		(4%)	(-9%)		(-24%)	(-8%)
2	140	177	121	0.19	0.15	0.19
		(26%)	(-14%)		(-24%)	(-1%)
3	119	174	137	0.15	0.14	0.17
		(46%)	(15%)		(-7%)	(16%)
4X[1]	31	11	10	0.48	0.60	0.63
		(-65%)	(-68%)		(25%)	(31%)
4X[2]	31	29	29	0.48	0.62	0.65
		(-6%)	(-6%)		(29%)	(35%)
4Y	80	84	78	0.37	0.47	0.56
		(5%)	(-3%)		(27%)	(51%)

[1] Dynamic characteristics from approximate formulas.

[2] Dynamic characteristics from modal analysis.

Examples 3 and 4 were non-planar walls and the response of the analysis models included torsional effects. Table 8 compares the torsional increase in displacements from the time history analysis with the increases recommended from the design procedure. These comparisons highlight the approximate nature of the design procedure. The increase was conservative for Example 3 (walls of different length on each

elevation) and Example 4 in the Y direction (U-shaped wall with load parallel to flanges, where there is no actual eccentricity). The increase was non-conservative for Example 4 in the X direction, the U-shaped wall loaded parallel to the web.

Table 8. Torsional Increase in Displacements Predictions from Design Procedure and Increase from Time History Analysis.

No.	Time History	Design Procedure
3	26%	58%
4X	39%	28%
4Y	2%	10%

8. RESPONSE VERSUS DUCTILITY FACTOR

The extent of rocking depends on the ductility factor, that is, the ratio of elastic seismic load to the lateral load causing uplift of the wall. As discussed earlier in this paper, New Zealand codes prior to NZS1170 permitted uplift provided the ductility factor associated with this uplift did not exceed 2. In this section, the impact of ductility factors up to 2 on response is assessed.

8.1 Displacements

The design procedure was used to develop curves for the ratio of rocking displacement to the non-rocking displacement, as plotted in Figure 33. The ratio of displacements for a range of initial elastic periods and all soil classes are plotted against the elastic period in this figure. All curves on Figure 33 assumed rocking will occur at a load level of 0.5 C(T), where C(T) is the elastic spectrum coefficient for horizontal loading. This is the definition of Ductility Factor 2 (DF 2).

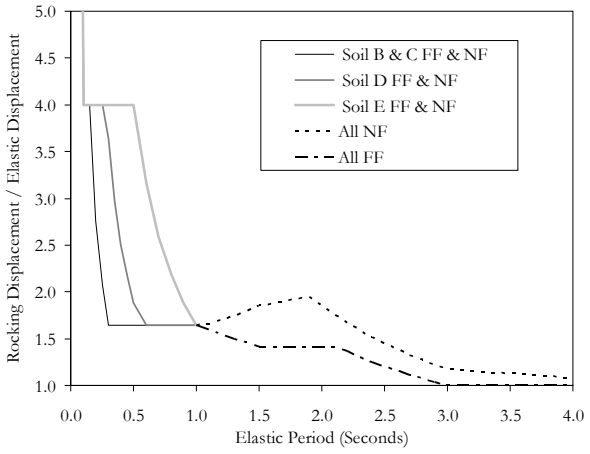

Figure 33. Effect of Soil Class on Rocking Displacements at DF 2.

The curves in Figure 33 are plotted separately for sites > 100 km from active faults (FF) and for sites within 2 km of active faults (NF):

1 The rocking displacements are greater than or equal to the elastic displacements in all cases. That is, the effect of rocking is never to reduce displacements.

2 For short periods, a rocking structure will have displacements 4 times that of a non-rocking structure. This applies for periods in the range of 0.10 to 0.15 for soil types B & C, 0.10 to 0.25 for soil type D and 0.10 to 0.50 for soil type E.

3 The ratio of rocking to elastic displacements reduces from 4.0 to a value of 1.64 at periods of 0.30 seconds (soils B & C), 0.60 seconds (soil D) and 1.0 seconds (soil E). The ratio remains at 1.64 up to a period of 1.0 seconds for all soil types. The curves are identical for both FF and NF locations up to this 1.0 second period.

4 For elastic periods greater than 1.0 seconds at FF sites the ratio of rocking to elastic displacement continues to decrease until the displacements are the same (ratio = 1.0) for periods of 3 seconds or longer, the constant displacement period of the NZS1170 spectra.

5 For elastic periods greater than 1.0 seconds at NF sites the ratio of rocking to elastic displacement increases from 1.64 to reach a peak ratio of 1.95 at a period of 1.90 seconds for all soil types. After the 1.90 second period the ratio decreases until the displacements are the same (ratio = 1.0) at periods of 5 seconds or longer. Although the near fault factor only applies for periods exceeding 1.50 seconds, the rocking displacements are affected from elastic periods greater than 1.0 seconds because at this elastic period the effective period of a DF 2.0 system is 1.50 seconds.

8.2 Dynamic Amplification Factors

The equations for dynamic shear amplification due to rocking, as a function of the ductility factor, are higher than those specified by NZS3101 for ductile walls. Figure 34 compares the dynamic amplification factors for rocking and ductile walls for varying number of stories, all for ductility factor 2.

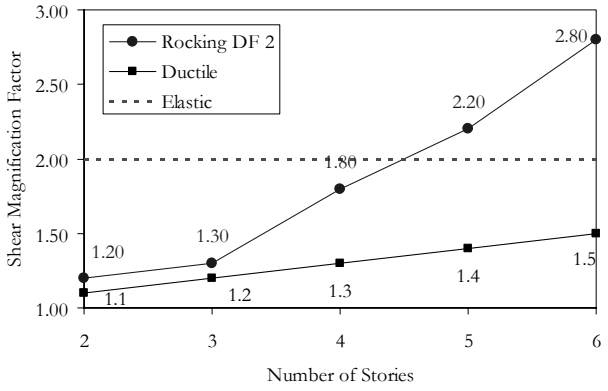

Figure 34. Comparison of Ductile Structure and Rocking Structure Amplification Factors.

NZS3101 specifies a constant amplification factor for ductile walls, varying only with the number of stories. Figure 34 shows that for a DF of 2, the amplification for rocking walls increases more rapidly than for ductile walls. The rocking amplification factors are only about 10% higher than for ductile walls for 2 and 3 storey walls but for walls of 4 stories or more the factors are much higher, reaching a value 87% greater for 6 storey walls.

The shear magnification factor is applied to the force required to initiate rocking, which by definition is one-half the elastic force for ductility factor 2. Therefore, the elastic force in the wall corresponds to a shear magnification factor of 2, the horizontal line plotted on Figure 34. Use of the elastic (non-rocking) shear force for design will be conservative for walls 4 stories or less in height.

8.3 Summary of Rocking at Ductility Factor 2

Uplift at load levels corresponding to one-half the design load level, equivalent to DF 2, influences both the displacements and shear forces:

1 Displacements are equal to or higher for a rocking structure than for an equivalent non-rocking system. The increase in displacements is greatest for structures on stiff springs (e.g. rock sites), where the displacements may be 4 or more times higher. However on such stiff sites the displacements are generally small so the amplification of displacements may not have much effect. For soft springs, such that the elastic period is 1 second or more, rocking displacements are up to 1.64 times the elastic displacements for sites distant from a fault and up to 2.0 times higher at near fault locations.

2 Shear force increases by dynamic amplification factors are higher for rocking walls than for ductile walls. At DF equal to 2 the increase is less than 10% for 2 or 3 storey structures but increases with height to an increase of 87% for 6 storey structures. For structures higher than 4 stories the shear force may exceed the elastic force.

9. FUTURE RESEARCH REQUIREMENTS

The research on rocking structures on which these guidelines were based served to illustrate the complexity of response of what appear to be relatively simple rocking systems. A number of outstanding issues were identified. Some of these items will be clarified by research programs already being progressed; others would justify additional research effort.

1 Shear amplification factors could be improved using statistical techniques such as the reliability index.

2 The procedure is not as accurate for wall configurations with significant torsion and the resistance mechanism is not well understood.

3 The method for calculating the period of rocking walls may be able to be extended to configurations with a torsional component.

4 The guidelines were developed using models with linearly elastic compression only soil springs, even though it is known that soil plasticity will modify response. Appropriate ways to model soil nonlinearity would improve the results.

5 Foundation pressures will be influenced by impact effects as the gap closes at speed. Design office type modelling with vertical mass results in high frequency vibrations of individual springs and does not take account of important items such as the continuum nature of the soil springs which couples response of the springs; radiation damping which acts to reduce impact forces and soil-structure interaction where the response of the rocking wall modifies the input. Further research is required.

6 Frame structures form another subset of uplifting structures, where exterior and corner columns may uplift. Future research should extend these procedures to assess whether they can be extended to include framed structures.

10. CONCLUSIONS

This paper has presented tentative design guidelines for rocking structures based on the results of an EQC funded research study. The guidelines are tentative in that important aspects of the response of rocking structures, such as soil plasticity and impact forces, were not included in their development. It is expected that further research will enable these guidelines to be refined.

The basis for the development of the guidelines was an extensive series of time history analyses of single wall models and a more limited series of models of multiple wall models. Findings from this research were:

1 Time history analysis using the mean response from seven frequency scaled earthquake records smoothed the nonlinear response and removed the variability associated with use of maximum values from three amplitude scaled records, the more usual procedure in New Zealand.

2 The displacement of single rocking walls was highly nonlinear once rocking occurred. Displacements in some cased exceeded five times the equivalent elastic displacements. Displacements were also 30% to 50% higher than those for an equivalent yielding wall.

3 The rocking strength of the wall limited base shear demand in single storey walls. For multi-story walls dynamic amplification, which was a strong function of ductility, increased the base shear demand.

4 Design office practice for nonlinear analysis is to exclude vertical mass. Because of this, impact forces are not developed due to gap closing. A limited number of analyses with vertical mass included showed large impact forces when the structure was founded on stiff springs. However, these forces would be alleviated by effects not included in the analysis such as soil yielding and radiation damping.

5 A procedure to estimate displacements in single walls, based on an effective period to define a substitute elastic structure, was found to be able to accurately predict displacements when the effective period was calculated as a function of the ductility factor.

6 The procedure could also provide reasonable estimates of displacement for multiple wall models but as the eccentricity of the wall configurations increased the accuracy of the predictions decreased.

7 A step-by-step procedure was developed to assess the displacements and shear forces in rocking wall structures. The procedure was implemented using standard office spreadsheet procedures. Four worked examples showed that the design procedure produced a reasonable match to time history results although the correlation reduced as the wall configurations became more complex.

Previous versions of the NZ loading code permitted uplift provided the ductility factor (DF) was not more than 2. This study showed that the effect of DF 2 was to increase displacements compared to elastic response, although generally by a factor of less than 2. Wall shear forces were also increased but not higher than for an equivalent wall which did not rock for walls 4 stories or less in height. This suggests that DF2 could be permitted in design for structures not more than four stories high with two conservative provisions:

1 Displacements calculated from the elastic model be increased by a factor of 2.0 for periods greater than 0.30 seconds for Soils A, B & C, 0.60 seconds for Soil D and 1.0 seconds for Soil E. If the period is less than this value then increase the displacements by a factor of 4.0.

2 The design shear forces are taken as the elastic shear force in the wall.

11. ACKNOWLEDGMENTS

The research on which this paper was based was financed by the EQC Research Foundation, Project OPR4. The author would like to thank Dr. Hugh Cowan, Research Manager at EQC, for his assistance in developing the project proposal and scope, and also Ms. Priscilla Cheung of EQC for her assistance with the administrative aspects of the project. Graham Voysey of the Holmes Consulting Group Auckland office provided valuable information relating to current design office practice and Bruce Galloway of the Christchurch office provided helpful review comments.

The author would also like to thank Quincy Ma for his many helpful review comments which improved the content and readability of this paper.

12. REFERENCES

1 Standards New Zealand, (1992). "Code of Practice for General Structural Design and Design Loadings for Buildings, NZS 4203:1992", *Standards New Zealand*.

2 Standards New Zealand, (2002). "Structural Design Actions, Parts 5 Earthquake Actions – New Zealand,, NZS1170.5:2004", *Standards New Zealand*.

3 Huckelbridge, A. A. (1977), "Earthquake Simulation Tests of a Nine Story Steel Frame with Columns Allowed to Uplift", *Earthquake Engineering Research Center,* Berkeley, CA, Report No. UCB/EERC-77-23.

4 Beck, J.L. and Skinner, R.I. (1974), "Seismic Response of a Reinforced Concrete Bridge Pier Designed to Step", *Earthquake Engineering & Structural Dynamics*, Vol. **2** No. 4.

5 Priestley, M.J.N., Evison, R.J. and Carr, A.J. (1978), "Seismic Response of Structures Free to Rock on Their Foundations", *Bulletin of the New Zealand National Society for Earthquake Engineering*, Vol. **11**, No. 3, September.

6 ASCE, American Society of Civil Engineers, (2000), "Prestandard and Commentary for the Seismic Rehabilitation of Buildings", *Federal Emergency Management Agency FEMA-356*, Washington, D.C.

7 Makris, N. and Konstantinidis, D. (2001), "The Rocking Spectrum and the Limitations of Design Guidelines", PEER Report 2005/04 *Pacific Earthquake Engineering Research Center College of Engineering University of California*, Berkeley, August.

8 Kelly, T.E. (2008), "Development of Design Guidelines for Rocking Structures", *EQC Research Foundation* Project OPR4, Holmes Consulting Group.

9 Housner, G.W. (1963), "The behaviour of Inverted Pendulum Structures During Earthquakes", *Bulletin of the Seismological Society of America*, Vol.**53**, No.2.

10 Yim, C.S., Chopra A.K. and Penzien, J. (1980), "Rocking Response Of Rigid Blocks To Earthquakes", *Earthquake Engineering and Structural Dynamics*, Vol. 8, 565-587.

11 Ishiyama, Y. (1982), "Motions Of Rigid Bodies And Criteria For Overturning By Earthquake Excitations", *Earthquake Engineering and Structural Dynamics*, Vol. **10**, 635-650.

12 Psycharis, I. N. (1982), "Dynamic Behavior of Rocking Structures Allowed to Uplift", EERL Report 81-02, *California Institute of Technology*, Pasadena, California.

13 Ma, Q., Wight, G.D., Butterworth, J. and Ingham, J.M. (2006), "Assessment of Current Procedures for Predicting the In-Plane Behaviour of Controlled Rocking Walls", *Proceedings of the 8th U.S. National Conference on Earthquake Engineering*, San Francisco, California.

14 ElGawady, M.A., Ma, Q., Butterworth, J. and Ingham, J.M. (2006), "The Effect of Interface Material on the Dynamic Behaviour of Free Rocking Blocks", *Proceedings of the 8th U.S. National Conference on Earthquake Engineering*, San Francisco, California.

15 Chung, M.A. and Larkin T.J. (2008), "Nonlinear Foundation Response of Liquid Storage Tanks under Seismic Loading", *Proceedings of New Zealand Society for Earthquake Engineering Annual Conference*.

16 Toh, J.C.W. and Pender, M.J. (2008), "Earthquake Performance and Permanent Displacements of Shallow Foundations", *Proceedings of New Zealand National Society for Earthquake Engineering Annual Conference*.

17 Harden, C., Hutchinson, T., Martin, G. and Kutter, B.L. (2005), "Numerical Modeling of the Nonlinear Cyclic Response of Shallow Foundations", PEER Report 2005/04 *Pacific Earthquake Engineering Research Center College of Engineering University of California, Berkeley,* August.

18 Kutter, B.L., Martin, G., Hutchinson, T., Harden, C., Gajan, S. and Phalen, J. (2006), "Workshop on Modeling of Nonlinear Cyclic Load-Deformation Behavior of Shallow Foundations", PEER Report 2005/14 *Pacific Earthquake Engineering Research Center College of Engineering University of California, Berkeley,* March.

19 Harden C.H. and Hutchinson, T. (2007), "Beam-on-Nonlinear-Winkler-Foundation Modeling of Shallow Rocking-Dominated Footings", *SEAOC 2007 Convention* Proceedings.

20 Anderson, D.L. (2003), "Effect of Foundation Rocking on the Seismic Response of Shear Walls", *Canadian Journal of Civil Engineering*, **30**:360-365.

21 Mondkar, D.P. and Powell, G.H. (1979),"ANSR II Analysis of Non-linear Structural Response User's Manual", EERC 79/17, *University of California, Berkeley,* July.

22 ATC (1996), "ATC Seismic Evaluation and Retrofit of Concrete Buildings", *Applied Technology Council, California*.

23 Standards New Zealand, (1995). "Concrete Structures Standard Part 1 – The Design of Concrete Structures" also "Part 2 – Commentary", NZS 3101:1995", *Standards New Zealand*.

24 Kelly, T. E. (2007), "A Blind Prediction Test Of Nonlinear Analysis Procedures For Reinforced Concrete Shear Walls", *Bulletin of the New Zealand Society for Earthquake Engineering*, Vol. **40**, No. 3.

APPENDIX A: DESIGN EXAMPLES

A.1 Single Wall

Design Conditions

This example considers a single storey wall 3.600 m long by 3.600 m high founded on medium to dense gravel. The total seismic weight at 1st floor level is 2,080 kN, which includes the self weight of the walls.

It is assumed that there are two walls arranged symmetrically in each direction to resist both gravity and seismic loads. The seismic load on each wall is 1040 kN and the gravity load on each wall is one-half the seismic weight, 520 kN. The wall is designed for these loads.

The foundation material has a shear modulus G = 60,000 kPa, a Poisson's ratio υ = 0.35 and a ULS strength q_c = 500 kPa. As the wall is single storey, the coefficients $C_m = C_0 = 1.0$.

The wall is located in a high seismic zone with:

Hazard Factor, Z	0.40
Return Period Factor, R	1.00
Site Subsoil Class	C
Structural Performance Factor, S_p	0.70
Distance to Fault	> 20 km

Step 1: Foundation Size

The wall is founded on a shallow foundation the same length as the wall, 3.600 m. From Equation 8, the minimum width is:

$$B > \frac{W}{q_c L} > \frac{520}{500 \times 3.6} = 0.289\,m$$

For Z=0.40 Class C the peak spectral acceleration is 0.820 and so the elastic seismic shear force V_E = 0.820 x 1040 = 853 kN.

For a given foundation width, B, the rocking load, V_R, can be calculated by replacing V_E with V_R in Equation 7 and re-ordering in terms of this variable:

$$V_R = \frac{WC_0}{2Bq_cH}(Bq_cL - W) \qquad \text{(A1)}$$

For this wall, a foundation width of 1.000 m is selected and the rocking capacity calculated as:

$$V_R = \frac{520 \times 1.0}{2 \times 1.000 \times 500 \times 3.6}(1.000 \times 500 \times 3.6 - 520) = 185kN$$

As the maximum elastic shear is 853 kN, this implies a ductility factor DF = 853 / 185 = 4.61. This is slightly higher than the preferred upper limit of 4 for which this procedure is intended but the wall is single storey and so will not be subject to dynamic amplification effects.

Step 2: Soil Spring Stiffness

It is assumed that there are seven distributed springs under the wall, as shown in Figure A1. This number was selected in order to match the models used for the time history analyses. A realistic minimum number would be five, two end springs plus three internal springs.

Based on the FEMA 356 soil spring model (see Figure 1) the spring spacing is as shown in Figure A1. The spacing of the end zones, L_1 = B/6 = 0.167 m and the spacing of the internal springs is L_2 = (3.600 – 2 x 0.167) / 5 = 0.653 m.

The spring stiffness of the end zone springs is calculated as

$$K_1 = k_{end}L_1 = \frac{6.83G}{1-\upsilon}L_1 = \frac{6.83 \times 60000}{1-0.35}0.167 = 105{,}077$$

And the stiffness of the internal springs as:

$$K_2 = k_{mid}L_2 = \frac{0.73G}{1-\upsilon}L_2 = \frac{0.73 \times 60000}{1-0.35}0.653 = 44{,}025$$

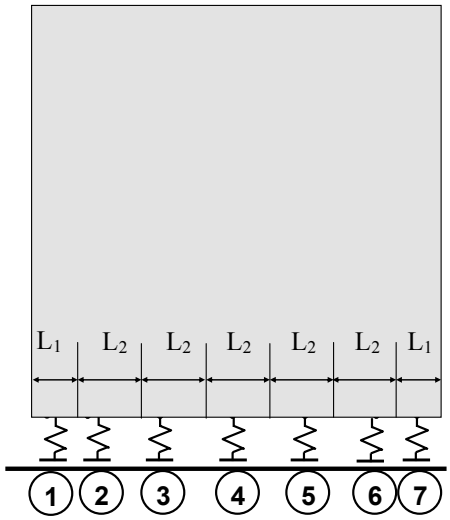

Figure A1 Soil Spring Layout Used for Design Examples.

The gravity load on each spring is calculated by assuming that the wall deforms uniformly such that the deflection of each spring is the same and the loads are distributed according to the spring stiffness as in Equation A2.

$$W_i = W\frac{K_i}{\sum K_i} \qquad \text{(A2)}$$

Table A1 lists the calculations to determine the reaction force at each spring location, the location of the wall centroid and the sum of spring inertia to calculate the period of the rocking wall. As this is a single wall, the location of the centroid $\bar{x}$ is at the mid-point of the wall, 1.800 m.

Table A1. Calculation of Single Wall Properties.

	x	K	W	Wx	x- $\bar{x}$	K(x- $\bar{x}$)^2
1	0.08	105077	127	11	-1.72	309656
2	0.49	44025	53.2	26	-1.31	75167
3	1.15	44025	53.2	61	-0.65	18792
4	1.80	44025	53.2	96	0.00	0
5	2.45	44025	53.2	131	0.65	18792
6	3.11	44025	53.2	165	1.31	75167
7	3.52	105077	127	447	1.72	309656
Sum		430277	520	936		807228

Step 3: Estimate Period

This wall has a single mass and so the mass moment of inertia about the base to calculate the period is 3.600^2 x 1040 / 9.81 = 1,374. The period is calculated using the definitions from Figure 5 as:

$$T = 2\pi\sqrt{\frac{M_R}{K_R}} = 2\pi\sqrt{\frac{1374}{807228}} = 0.259\ Seconds$$

A wall of this configuration was analysed and the period as reported in [8] was 0.269 seconds, within 5% of the value calculated above.

Step 4: Compression Block Size

The length of the compression block is

$$c = \frac{W}{q_c B} = \frac{520}{500 \times 1.000} = 1.040\ m$$

Step 5: Calculate Wall Rocking Strength

The yield force

$$F_y = \frac{W(\frac{L}{2} - \frac{c}{2})}{\frac{H}{C_0}} = \frac{520(\frac{3.600}{2} - \frac{1.040}{2})}{\frac{3.600}{1.0}} = 185\ kN$$

The yield coefficient is:

$$C_y = \frac{F_y}{Mg} = \frac{185}{1040} = 0.178$$

Step 6: Calculate Seismic Displacement

The seismic displacement is calculated from the effective period and requires a recursive solution. Table A2 shows a procedure for solving for T_e using spreadsheet equations:

1 Assume a period, T_i. For step 1, this is the elastic period, T_1. For subsequent steps, set $T_i = 0.5$ x $(T_i + T_e)^{i-1}$ where the sum $(T_i + T_e)^{i-1}$ is of values from the preceding step.

2 Calculate the design coefficient at T_i, $C(T_i)$, from the NZS1170 equations.

3 The response modification factor, $R_e = C_m C(T_i) / C_y$.

4 The new effective period is $T_e = R_e T_i$.

5 Calculate the ratio T_i / T_e and repeat until this ratio equals unity, within a specified tolerance.

In Table A2, five iterations produce convergence to three decimal places and an effective period of 0.662 seconds.

Table A2. Calculation of Single Wall Effective Period.

1. T_i	2. $C(T_i)$	3. R_e	4. T_e	5. T_e/T_i
0.259	0.820	4.615	1.196	4.619
0.728	0.423	2.377	0.616	0.847
0.672	0.449	2.524	0.654	0.974
0.663	0.453	2.549	0.661	0.997
0.662	0.454	2.552	0.662	1.000

At the effective period of 0.662 seconds the design coefficient C = 0.454. The displacement of the equivalent single degree of freedom is calculated from Equation 13 as

$$\Delta = C(T_e) g \frac{T_e^2}{4\pi^2} = 0.454 \times 9810 \times \frac{0.662^2}{4\pi^2} = 49.4\ mm$$

As the wall is single storey C_0 = 1.0 and the top of wall displacement is equal to the calculated spectral displacement of 49.4 mm.

Step 7: Calculate Ductility Factor

$$DF = \frac{C(T_1)}{C_Y} = \frac{0.820}{0.178} = 4.615$$

Step 8: Assess Dynamic Amplification Effects on Wall Shear

Dynamic amplification is a higher mode effect and so does not occur in a single storey wall such as this example.

Step 9: Calculate Torsional Increase in Displacements

Torsion effects are not included in a single wall example.

Step 10: Assessment of Performance

Assuming this wall did not rock, the spectral displacement can be calculated from the elastic coefficient at the initial period T_1 as:

$$\Delta = C(T_1) g \frac{T_1^2}{4\pi^2} = 0.820 \times 9810 \times \frac{0.259^2}{4\pi^2} = 13.67\ mm$$

The design procedure shows that the wall will rock with a maximum displacement of 49.4 mm, which is 3.6 times as higher as the elastic displacement. As the wall is a single storey the shear force will be limited to the force required to initiate rocking, 185 kN, compared to 853 kN for the non-rocking wall.

The drift angle is calculated using NZS1170 requirements as $\delta = k_{dm}\Delta/H$ = 1.2 x 49.4 / 3600 × 1.65%, which is about two-thirds the code limit of 2.50%. Therefore, the wall performance will be satisfactory.

Comparison with Time History Results

This example wall configuration corresponds to the wall for which time history results are plotted in Figure 24 of this paper. For the time history analysis S_p = 1.0 and so ZS_p = 0.28 corresponds to the results for ZR = 0.28 far fault Soil C. The mean result from the seven time histories was 46.8 mm, which is within 5% of the value of 49.4 mm predicted from the design procedure. However, the design base shear coefficient of 0.178 (equal to the yield coefficient for this single storey wall) is 24% less than the time history coefficient of 0.233.

The design was repeated using the failure strength of $2q_c$, as this corresponds more closely to the results of time history which are performed using actual strengths. With this strength, both the displacement and base shear coefficient were within 10% of the time history value, as listed in Table A3.

Table A3. Comparison of Design Procedure Results with Time History Results for Single Wall.

	Displacement Δ (mm)	Base Shear Coefficient, C
Time History Analysis	47	0.233
Design Procedure	49	0.178
Design Procedure, $2q_c$	43	0.214

A.2 Two Planar Walls

Design Conditions

This example considers a symmetric layout of three storey walls where each elevation comprises of one 7.200 m long wall and one 3.600 m long wall, as shown in Figure A2. The walls are founded on medium gravel. The seismic weight

tributary to the walls at each of the three floor levels is 2030 kN, which includes the self weight of the walls.

It is assumed that the walls are arranged symmetrically on the other side of the building so that there is no torsion. (The effect of torsion is considered in Example 3). The weight on each wall is the same, 515 kN per floor so that the two walls together have a total vertical load equal to one-half the seismic weight. This assumes that one-half the gravity loads are supported by the structure in the orthogonal direction.

The foundation material is the same as for Example 1, with a shear modulus G = 60,000 kPa, a Poisson's ratio υ = 0.35 and a ULS strength q_c = 500 kPa. For a three storey wall, FEMA 356 provides coefficients C_m = 0.80 and C_0 = 1.2.

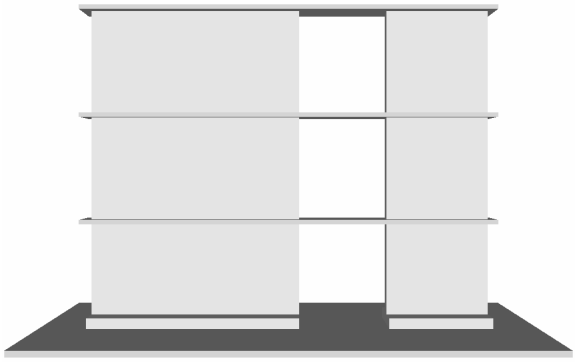

Figure A2. Example 2, Multiple Planar Walls.

The wall is located in a near fault, high seismic zone with factors:

Hazard Factor, Z	0.40
Return Period Factor, R	1.00
Site Subsoil Class	C
Structural Performance Factor, S_p	0.70
Distance to Fault	< 2 km

Step 1: Foundation Size

Each wall is founded on a shallow foundation the same length as the wall. From Equation 8, the minimum width is:

$$B > \frac{W}{q_c L} > \frac{515 \times 3}{500 \times 7.2} = 0.429\, m \text{ for Wall } 1$$

$$B > \frac{W}{q_c L} > \frac{515 \times 3}{500 \times 3.6} = 0.858\, m \text{ for Wall } 2$$

As for Example 1, the foundation width was set at 1.000 m for both walls and the performance assessed.

Step 2: Soil Spring Stiffness

The distributed spring layout shown in Figure A1 was used for each of the two walls and the stiffness calculated in a similar fashion. Table A4 lists the calculations, which are similar to those for Table A1 except that the two walls are assessed independently.

Step 3: Estimate Period

This wall has a multiple mass and so the mass moment of inertia about the base, used to calculate the period, is calculated as in Table A5. The period is calculated using the definitions from Figure 5 as:

$$T = 2\pi\sqrt{\frac{M_R}{K_R}} = 2\pi\sqrt{\frac{37546}{(4{,}344{,}335 + 807{,}228)}} = 0.536 \text{ Seconds}$$

A wall of this configuration was analyzed and the period as reported in [8] was 0.568 seconds, about 6% higher than the calculated value. When the analysis model was modified so that the wall was rigid the period reduced to 0.537 seconds, almost identical to the value calculated here.

Table A4. Calculation of Two Planar Wall Properties.

	x	K	W	Wx	x- $\bar{x}$	K(x- $\bar{x}$)^2
1	0.08	105077	241.3	20	-3.52	1299480
2	0.85	92542	212.5	181	-2.75	698150
3	2.23	92542	212.5	473	-1.37	174537
4	3.60	92542	212.5	765	0.00	0
5	4.97	92542	212.5	1057	1.37	174537
6	6.35	92542	212.5	1349	2.75	698150
7	7.12	105077	241.3	1717	3.52	1299480
Sum		672862	1545	5562		4344335
1	0.08	105077	377.3	31	-1.72	309656
2	0.49	44025	158.1	78	-1.31	75167
3	1.15	44025	158.1	181	-0.65	18792
4	1.80	44025	158.1	285	0.00	0
5	2.45	44025	158.1	388	0.65	18792
6	3.11	44025	158.1	491	1.31	75167
7	3.52	105077	377.3	1327	1.72	309656
Sum		430277	1545	2781		807228

Table A5. Mass Moment of Inertia.

Height, h	Mass, M	Mh^2
10.800	207	24137
7.200	207	10727
3.600	207	2682
Sum	621	37546

Step 4: Compression Block Size

The length of the compression block is the same for both walls and is calculated as:

$$c = \frac{W}{q_c B} = \frac{1545}{500 \times 1.000} = 3.090\ m$$

Step 5: Calculate Wall Rocking Strength

The yield force is calculated separately for each wall:

$$F_{y1} = \frac{W(\frac{L}{2} - \frac{c}{2})}{\frac{H}{C_0}} = \frac{1545(\frac{7.200}{2} - \frac{3.090}{2})}{\frac{10.800}{1.2}} = 353\ kN$$

$$F_{y2} = \frac{W(\frac{L}{2} - \frac{c}{2})}{\frac{H}{C_0}} = \frac{1545(\frac{3.600}{2} - \frac{3.090}{2})}{\frac{10.800}{1.2}} = 44\ kN$$

The yield coefficient is based on the summation of rocking forces in both walls:

$$C_y = \frac{F_y}{Mg} = \frac{(353+44)}{6090} = 0.065$$

Step 6: Calculate Seismic Displacement

Table A6 implements the same iterative procedure as for Example 1, with subsequent iterations using the average period from the preceding iteration. In Table A6, seven iterations produced convergence within three decimal places and a final effective period of 1.575 seconds.

Table A6. Calculation of Two Planar Walls Effective Period.

T_i	$C(T_i)$	R_e	T_e	T_e/T_i
0.536	0.531	6.527	3.501	6.527
2.019	0.206	2.529	1.357	0.672
1.688	0.229	2.812	1.508	0.894
1.598	0.237	2.908	1.560	0.976
1.579	0.239	2.930	1.572	0.995
1.575	0.239	2.935	1.574	0.999
1.575	0.239	2.935	1.574	1.000

At the effective period of 1.575 seconds the design coefficient $C(T_e)$ = 0.239. The displacement of the equivalent single degree of freedom is calculated from Equation 13 as

$$\Delta = C(T_e) g \frac{T_e^2}{4\pi^2} = 0.239 \times 9810 \times \frac{1.575^2}{4\pi^2} = 147 \ mm$$

The top of wall displacement equals the calculated spectral displacement times C_0, i.e. 147 x 1.2 = 177 mm.

Step 7: Calculate Ductility Factor

$$DF = \frac{C(T_1)}{C_Y} = \frac{0.531}{0.065} = 8.2$$

Step 8: Assess Dynamic Amplification Effects on Wall Shear

The dynamic amplification factor is calculated from Equation 19a. From Table 4, the coefficient for a three storey structure is 0.15 and so the omega factor is calculated as:

$$\omega_V = 1 + a_{VN} DF = 1 + 0.15 \text{ x } 8.2 = 2.23 \leq 0.5 + N = 3.5$$

Therefore, the design shear forces are amplified by a factor of 2.23.

Step 9: Calculate Torsional Increase in Displacements

Torsion effects are not included in this example.

Step 10: Assessment of Performance

The drift angle is 1.2 x 177 / 10,800 = 1.97%, within the code limit of 2.50%. Although this is within the allowable limit, assume that design criteria restrict maximum drift to 1%. Table A7 documents the effect on the drift and the design shear force by increasing the foundation width from 1.000 m to 3.000 m:

1 The displacement, and therefore drift, decreases with increases in foundation width. If the foundation width is tripled, from 1.0 m to 3.0 m, the drift is reduced by 50%, from 1.97% to 0.97%.

2 As the drift reduces, the design shear force increases. This is despite a reduction in ductility factor (from 8.2 to 5.5) and a reduction in dynamic amplification factor (from 2.22 to 1.83). The reason for this is that the rocking strength is proportional to the foundation width and an increase in width from 1.0 m to 3.0 m increases the rocking coefficient by almost 90%, from 0.065 to 0.123.

Table A7. Effect of Increasing Foundation Width.

B	C_y	DF	Δ	ω_v	Drift	$V=C_y \omega_v$
1.000	0.065	8.2	177	2.22	1.97%	0.144
1.250	0.083	6.7	141	2.01	1.57%	0.167
1.500	0.094	6.1	123	1.92	1.37%	0.180
2.000	0.109	5.7	105	1.85	1.17%	0.202
2.500	0.117	5.6	94	1.83	1.04%	0.214
3.000	0.123	5.5	87	1.83	0.97%	0.225

Comparison with Time History Results

The design coefficient ZS_p = 0.28 corresponds to time history results for ZR = 0.28 near fault Soil C. Table A8 compares the results from the design procedure with the time history results. As for Example 1, the design procedure calculations were repeated using the failure soil strength, $2q_c$.

The design procedure over-estimated displacements by 26% and under-estimated base shears by 24%. When the failure soil strength was used ($2q_c$) the displacements were under-estimated by 14% and shear forces under-estimated by only 1%.

Table A8. Comparison of Design Procedure Results with Time History Results for the Two Planar Walls.

	Displacement Δ (mm)	Base Shear Coefficient, C
Time History Analysis	140	0.190
Design Procedure	177	0.145
Design Procedure, $2q_c$	121	0.188

For a more complete comparison with time history results, the design procedure equations were used to predict displacements and base shear coefficient at all seismic amplitude levels for which the time histories were evaluated (seismic zone factor ZR = 0.07 to 0.70 at an increment of 0.07). Figure A3 compares the results at all amplitudes:

1 The design procedure based on the ULS soil strength, q_c, overestimates displacements. For low amplitudes the displacement predictions are close (within 5% at ZR = 0.07) but the discrepancy increases with amplitude. The design procedure predicted displacements 71% higher at ZR = 0.70. The shear coefficient from the design procedure is approximately 25% lower than the time history result for the full range of amplitudes.

2 When the design procedure calculations are based on the failure soil strength, $2q_c$, the displacements match the mean time history results much more closely, with less than 10% difference at most values. The base shear

coefficient similarly matches more closely, also within 10%.

These results suggest that the soil failure strength may be a better parameter than ULS strength in calculating a response to match time history values. Use of the ULS strength will tend to over-estimate displacements but be non-conservative for shear forces.

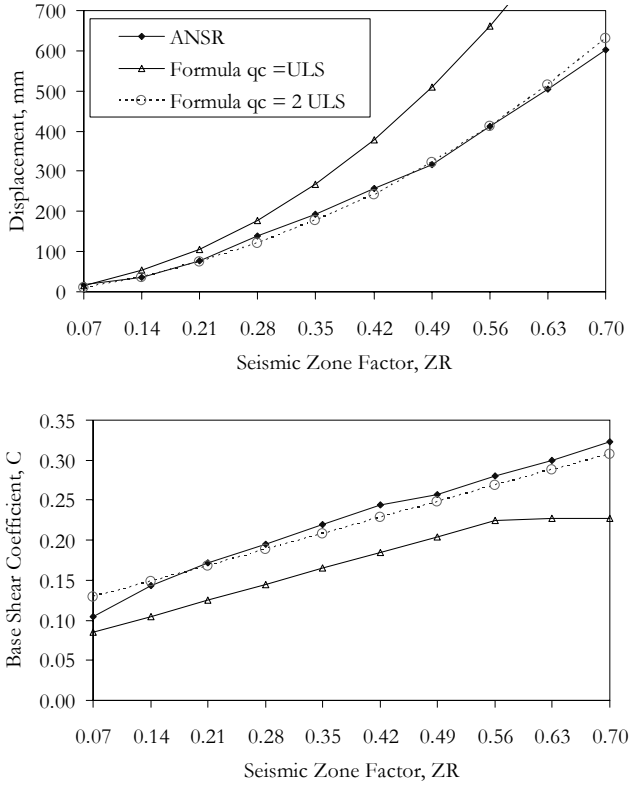

Figure A3. Effect of Ultimate Soil Spring Strength on (a) Predicted Displacements and (b) Base Shear Coefficient.

A.3 Two Non-Planar Walls

This example considers a non-symmetrical layout of walls such that there is a torsional component to the response. The example building, as shown in Figure A4, is a two storey square building with 3.600 m long walls on two adjacent elevations and 7.200 m long walls on the other two adjacent elevations.

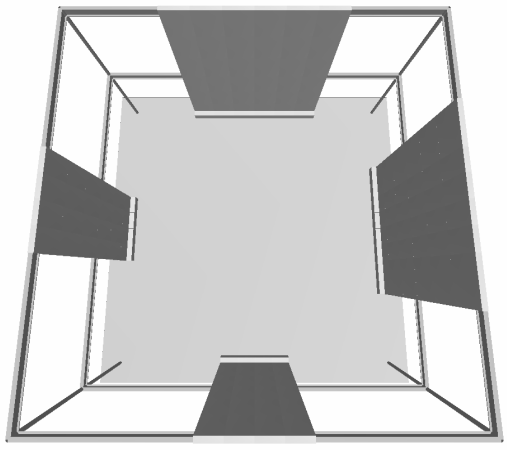

Figure A4. Analysis Model of Wall with Non-symmetrical Wall Layout.

The seismic weight at each of the two floor levels is 1,555 kN, which includes the self weight of the walls. The gravity load is distributed evenly along the four elevations of the building, equivalent to a uniform load of 27 kN/m (4 elevations x 14.400 m length x 27 = 1,555 kN). Part of the gravity load is supported by the corner columns, so that the loads on each of the walls are 479 kN and 576 kN for the 3.600 m and 7.200 m long walls respectively. (These values are the total loads including the two floor levels).

The foundation material is assumed to be a relatively soft material, medium clay, with a shear modulus G = 10,000 kPa, a Poisson's ratio $\upsilon = 0.50$ and a ULS strength q_c = 150 kPa. For a two storey wall, FEMA 356 provides coefficients C_m = 1.0 and C_0 = 1.2.

The wall is located in a near fault, high seismic zone with NZS 1170 factors:

Hazard Factor, Z	0.40
Return Period Factor, R	1.00
Site Subsoil Class	C
Structural Performance Factor, S_p	0.70
Distance to Fault	< 2 km

As is usual in design office practice, the structure was assessed for loads applied separately along the two orthogonal translational axes. In each direction, the wall has one 3.600 m and one 7.200 m wall and so the structural properties are equal. Therefore, only the evaluation for X axis loading is calculated here.

Step 1: Foundation Size

Each wall is founded on a shallow foundation, assumed to be the same length as the wall. From Equation 8, the minimum width is:

$$B > \frac{W}{q_c L} > \frac{479}{150 \times 3.6} = 0.887\, m \text{ for Wall } 1$$

$$B > \frac{W}{q_c L} > \frac{576}{150 \times 7.2} = 0.533\, m \text{ for Wall } 2$$

The foundation width was set at 1.500 m for both walls and the performance assessed.

Step 2: Soil Spring Stiffness

The distributed springs shown in Figure A1 were used for each individual wall. The wall properties were combined, using the coordinate numbering as shown in Figure A5. Properties were calculated for loads in the X direction, about an axis orthogonal to the load. Table A9 lists the calculations of spring properties. As the walls are symmetrically located about the building centroid, the distance to the centre of gravity is one-half the building dimension, 7.200 m.

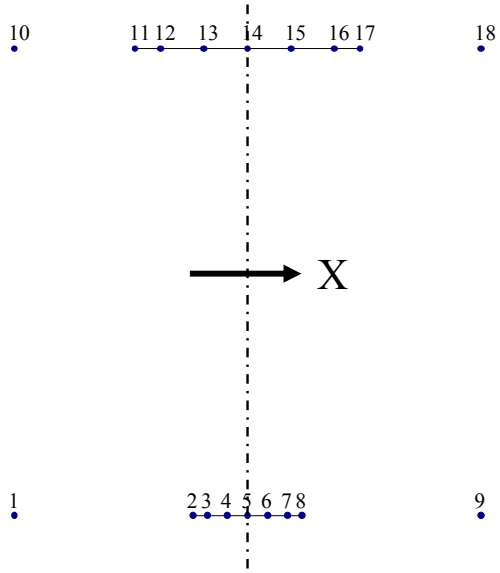

Figure A5. Coordinate Numbering for Calculation of Properties for Non-symmetrical Wall Layout.

Table A9. Calculation of Two Non-Planar Wall Properties

	x	K	W	Wx	x- $\bar{x}$	K(x- $\bar{x}$)^2
1	0	0	149.2	0	-7.20	0
2	5.525	34150	160.9	889	-1.68	95812
3	5.96	9052	28.5	170	-1.24	13918
4	6.58	9052	33.5	220	-0.62	3480
5	7.20	9052	33.5	241	0.00	0
6	7.82	9052	33.5	262	0.62	3480
7	8.44	9052	28.5	240	1.24	13918
8	8.88	34150	160.9	1428	1.68	95812
9	14.40	0	149.2	2148	7.20	0
10	0.00	0	100.6	0	-7.20	0
11	3.725	34150	122.0	455	-3.48	412383
12	4.520	19564	57.6	261	-2.68	140516
13	5.860	19564	72.4	424	-1.34	35129
14	7.200	19564	72.4	521	0.00	0
15	8.540	19564	72.4	618	1.34	35129
16	9.880	19564	57.6	570	2.68	140516
17	10.675	34150	122.0	1303	3.48	412383
18	14.400	0	100.6	1448	7.20	0
Sum		279680	1555	11197		1176056

Step 3: Estimate Period

The mass moment of inertia about the base, calculated in Table A10, is used to calculate the period using the definitions from Figure 5:

$$T = 2\pi\sqrt{\frac{M_R}{K_R}} = 2\pi\sqrt{\frac{10273}{1176056}} = 0.587 \; Seconds$$

A wall of this configuration was analysed and the first two fundamental periods as reported in [8] were 0.758 and 0.648 seconds. The lower of these is over 10% higher than the calculated value. The reason for this discrepancy is that the modes extracted from the analysis model were along the diagonal axis of the building, with significant effective mass factors along both axes.

Table A10. Mass Moment of Inertia.

Height, h	Mass, M	Mh^2
7.2	159	8218
3.6	159	2055
Sum	317	10273

Step 4: Compression Block Size

The length of the compression block is calculated for each of the two walls resisting loads in this direction as:

$$c = \frac{W}{q_c B} = \frac{479}{150 \times 1.500} = 2.13 \; m \;\; for \; Wall \; 1$$

$$c = \frac{W}{q_c B} = \frac{576}{150 \times 1.500} = 2.56 \; m \;\; for \; Wall \; 2$$

Step 5: Calculate Wall Rocking Strength

The yield force is calculated separately for each wall:

$$F_{y1} = \frac{W(\frac{L}{2} - \frac{c}{2})}{\frac{H}{C_0}} = \frac{479\,(\frac{3.600}{2} - \frac{2.13}{2})}{\frac{7.200}{1.2}} = 59 \; kN$$

$$F_{y2} = \frac{W(\frac{L}{2} - \frac{c}{2})}{\frac{H}{C_0}} = \frac{576\,(\frac{7.200}{2} - \frac{2.56}{2})}{\frac{7.200}{1.2}} = 223 \; kN$$

The yield coefficient is based on the summation of rocking forces in both walls:

$$C_y = \frac{F_y}{Mg} = \frac{(59 + 223)}{3110} = 0.091$$

Step 6: Calculate Seismic Displacement

Table A11 summarises the same iterative procedure as for Examples 1 and 2, with each subsequent step using the average period from the preceding step. Seven iterations produce convergence within three decimal places and an effective period of 1.560 seconds.

Table A11. Calculation of Two Non-Planar Walls Effective Period.

T_i	$C(T_i)$	R_e	T_e	T_e/T_i
0.587	0.496	5.484	3.221	5.484
1.904	0.213	2.353	1.382	0.726
1.643	0.233	2.571	1.510	0.919
1.576	0.239	2.638	1.549	0.983
1.563	0.240	2.653	1.558	0.997
1.560	0.240	2.655	1.559	0.999
1.560	0.240	2.656	1.560	1.000

At the effective period of 1.560 seconds the design coefficient $C(T_e)$ = 0.240. The displacement of the equivalent single degree of freedom is calculated from Equation 13 as:

$$\Delta = C(T_e)g\frac{T_e^2}{4\pi^2} = 0.240 \times 9810 \times \frac{1.560^2}{4\pi^2} = 145\ mm$$

The top of wall displacement equals the calculated spectral displacement times C_0, i.e. 145 x 1.2 = 174 mm.

Step 7: Calculate Ductility Factor

$$DF = \frac{C(T_1)}{C_Y} = \frac{0.496}{0.091} = 5.5$$

Step 8: Assess Dynamic Amplification Effects on Wall Shear

The dynamic amplification factor is calculated from Equation 19a. From Table 4, the coefficient for a two storey structure is 0.10 and so the omega factor is calculated as:

$$\omega_V = 1 + a_{VN}\,DF = 1 + 0.10 \text{ x } 5.5 = 1.55 \leq 0.5 + N = 2.5$$

Therefore, the design shear forces are amplified by a factor of 1.55.

Step 9: Calculate Torsional Increase in Displacements

The tentative design procedure suggests that centre of mass displacements be increased by a factor two times the calculated actual eccentricity, but not less than a factor equal to the code required accidental eccentricity (set at 0.10 in NZS1170).

For these two walls, the eccentricity can be calculated using either the weight resisted by each wall or the lateral load resisted by each wall. From the calculations above, the shorter wall supports a weight of 479 kN and has a rocking capacity of 59 kN. The longer wall supports 576 kN but has a rocking capacity of 223 kN. The weight eccentricity is calculated as

$$e = \frac{D}{2} - \frac{\sum W_i y_i}{\sum Wi} = \frac{14.4}{2} - \frac{(479 \times 0) + (576 \times 14.4)}{(479 + 576)} = -0.661m$$

The eccentricity measured as the distance of the centre of resistance from the centroid is calculated as:

$$e = \frac{D}{2} - \frac{\sum F_{yi} y_i}{\sum F_{yi}} = \frac{14.4}{2} - \frac{(59 \times 0) + (223 \times 14.4)}{(59 + 223)} = -4.187m$$

It would seem logical that displacements be related to the eccentricity of resistance and so for this wall the actual eccentricity is (4.187 / 14.400) = 0.291D. The increase due to eccentricity is 2 x 0.291 = 58%.

Table A12 lists displacements for this wall at the centre of mass (C of M) and the maximum value at any location. Results are listed for the analysis with no eccentricity and then plus and minus the code specified eccentricity of 0.10D.

Table A12. Displacements for Two Non-Planar Walls with Torsional Effects.

Location	Eccentricity	Displacement	Increase
C of M	None	119.2	
Maximum	None	125.5	5%
Maximum	+ 0.1 B	150.0	26%
Maximum	- 0.1B	119.9	1%

There is very little torsional increase when there is no eccentricity or negative eccentricity (the latter when the centre of mass is moved closer to the centre of resistance). With positive eccentricity the analysis displacements increase by 26%, less than one-half the design value of 58%.

Step 10: Assessment of Performance

The height of this wall is 7.200 m and the maximum displacement is 1.58 x 174 = 275 mm. This represents a drift angle of 1.2 x 0.275 / 7.200 = 4.58%, much greater than the allowable limit of 2.50%. One method of reducing the drift is to increase the length of the foundation under the shorter (3.600 m) wall, therefore reducing the torsion.

Table A13 summarises the calculated seismic displacement, Δ, and maximum displacement including torsion, Δ_m, for three different foundation lengths. The 3.600 m length implies a footing the same length as the wall, the 5.100 m and 6.600 m lengths imply that the footings cantilever respectively 0.750 m and 1.500 m from each end of the wall.

The increased foundation length increases the rocking strength of the shorter wall, which reduces the eccentricity of the centre of resistance. The increased foundation length also reduces the effective period and thereby the centre of mass displacement. The net effect of these is that increasing the foundation length of the shorter wall from 3.600 m to 6.600 m reduces the peak drift from 4.58% to 2.40%.

Table A13. Effect of Increasing Foundation Beam Length.

	Foundation Length Under 3.600 m Wall		
	3.600 m	**5.100 m**	**6.600 m**
Wall 1 F_y	59	121	192
Wall 2 F_y	223	223	223
e / B	0.29	0.15	0.04
Δ	174	149	131
Δ_m	275	194	144
Drift	4.58%	3.23%	2.40%

Comparison with Time History Results

Table A14 compares the design procedure prediction with the mean results from the time history analysis for the same level of seismic input. As for the preceding examples, the design procedure was repeated using the failure soil strength, $2q_c$.

Table A14. Comparison of Design Procedure Results with Time History Results for Two Non-Planar Walls.

	Displacements		Base Shear
	C of M	**Max.**	**Coefficient, C**
Time History Analysis	119	150	0.150
Design Procedure	174	275	0.140
Design Procedure, $2q_c$	137	216	0.174

The design procedure over-estimated centre of mass displacements by 46% and under-estimated base shears by 7%. When the failure soil strength was used ($2q_c$) the centre of

mass displacements were over-estimated by 15% and shear forces were over-estimated by 16%.

The torsional effect increase predicted by the design procedure, 58%, was higher than that recorded by the time history analyses. The maximum displacement predicted by the design procedure was also shown to be very conservative, 83% higher that the time history results when the ULS soil strength was used and 44% higher when the soil strength was increased to the failure strength of $2q_c$.

As for Example 2, the design procedure was used to develop the predicted displacements and base shear coefficient at all seismic amplitude levels for which the time histories were evaluated. Figure A5 compares the results without any allowance for torsion:

1 The design procedure based on the ULS soil strength, q_c, overestimates displacements by about 30% to 50% but estimates a base shear coefficient very close to the time history mean value, generally within 10%.

2 When the design procedure calculations are based on the failure soil strength, $2q_c$, the displacements match the time history mean results more closely, with less than 20% difference. However, the base shear coefficient is over-estimated by 15% to 20%.

These results suggest that for this wall the soil failure strength may be a better parameter than the ULS strength in calculating a response to match time history values, although it will be conservative for shear. The use of ULS strength will tend to over-estimate displacements but will provide a good estimate of shear forces.

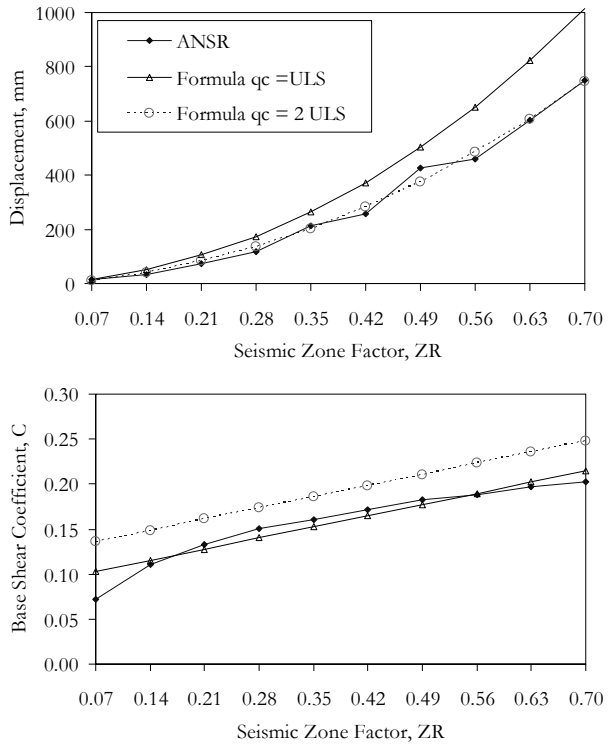

Figure A5. Effect of Ultimate Soil Spring Strength on (a) Predicted Displacements and (b) Base Shear Coefficient for Non-Planar Walls.

Torsion Displacements

The design procedure over-estimated torsional effects by a wide margin, as shown by the comparison in Table A14. The calculated eccentricity of the centre of resistance was 0.29D and it was expected that torsional increases in displacement would be relatively large.

Figure A6 plots the diaphragm displacements and the total displacements from the time history analyses and compares them with results from the design procedure using a soil strength of $2q_c$.

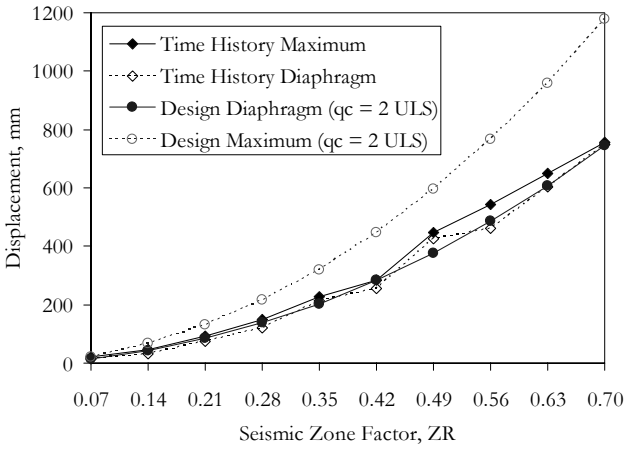

Figure A6. Total Displacements including Torsional Effects for Non-Planar Walls.

The diaphragm displacements are similar for both the time history analysis and the design procedure. However, the design procedure predicted maximum displacements 58% higher than the time history results at all amplitudes. Trends from the time history results for this structure are:

1 At low seismic amplitudes, ZR = 0.14, torsion increases displacements from 32.8 mm to 47.8 mm, an increase of 46%.

2 At moderate seismic amplitudes, ZR = 0.28, corresponding to the design condition for this example, the torsional effects increase displacements from 119 mm to 150 mm, an increase of 26%.

3 At very high seismic loads, ZR = 0.70, there is a very small increase in displacement due to torsion, from 750 mm to 757 mm which represents only a 1% increase.

This reaffirms the trend shown in Figure 26, which indicates that torsional effects reduce with increasing drift. This suggests that the torsional effects in rocking walls are complex and not within the scope of this study.

A.4 U-Shaped Wall

Example 4 is the U-shaped layout of walls shown in Figure A7. The example is a three storey rectangular building, 7.200 x 14.400 m in plan. As for many retail occupancies, the structure has solid walls on three sides and is open on the fourth side. Pinned columns at third points along the front face support part of the floor load but these columns do not contribute to the lateral strength of the building.

The seismic weight at each of the three floor levels is 778 kN, including the self weight of the walls. The floors span in the shorter (7.200 m) direction.. The walls support two-thirds of the total gravity load and the two internal front columns support the remaining one-third of the weight.

The foundation material is assumed to be a relatively soft material, medium clay, with a shear modulus G = 10,000 kPa, a Poisson's ratio $\upsilon = 0.50$ and a ULS strength q_c = 150 kPa. For a three storey wall, FEMA 356 provides coefficients C_m = 0.8 and C_0 = 1.2.

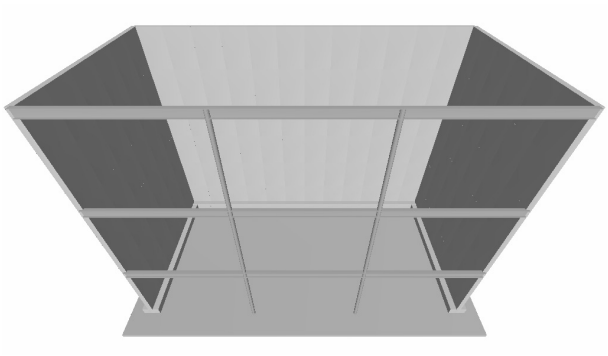

Figure A7. Analysis Model of Wall with U-Shaped Wall Layout.

The wall is located in a near fault, high seismic zone with NZS 1170 factors:

Hazard Factor, Z	0.40
Return Period Factor, R	1.00
Site Subsoil Class	C
Structural Performance Factor, S_p	0.70
Distance to Fault	< 2 km

As for usual design office practice, the structure was assessed for loads applied separately along the two orthogonal translational axes.

Step 1: Foundation Size

The total foundation length under the wall is 28.800 m and the total gravity load is 1555 kN (two-thirds the total weight of 778 kN x 3 floors). For an ultimate bearing strength of 150 kPa the minimum foundation width is

$$B > \frac{W}{q_c L} > \frac{1555}{150 \times 28.800} = 0.360\,m$$

As the foundation stiffness was low, the foundation width was set at 1.500 m and the performance was assessed for this condition.

Step 2: Soil Spring Stiffness

As for the other examples, the distributed springs shown in Figure A1 were used, with 4 internal nodes per wall segment. Each of the three wall segments was treated as a separate wall, using the coordinate numbering shown in Figure A8.

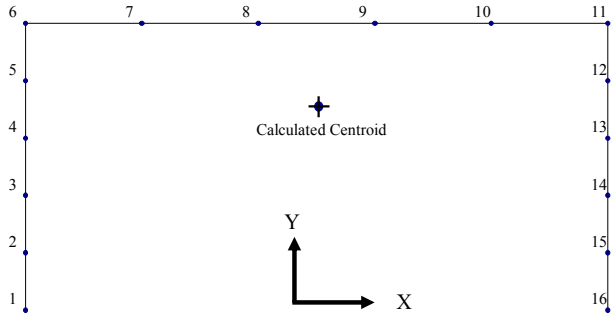

Figure A8. Coordinate Numbering for Calculation of Properties for U-Shaped Wall Layout.

The two flanges of the wall are each 7.200 m long. Based on FEMA 356's soil spring model the spacing of the end zones, L_1 = B/6 = 0.250 m.

The spacing of the internal springs was determined as

L_2 = (7.200 – 2 x 0.250) / 4 = 1.675 m.

For the flanges, the external spring stiffness values were calculated as:

$$K_1 = k_{end} L_1 = \frac{6.83G}{1-\upsilon} L_1 = \frac{6.83 \times 10000}{1-0.50} 0.250 = 34{,}150$$

The stiffness of the internal springs in the flange walls was:

$$K_2 = k_{mid} L_2 = \frac{0.73G}{1-\upsilon} L_2 = \frac{0.73 \times 10000}{1-0.50} 1.675 = 24{,}455$$

The web of the wall is 14.400 m long. The spacing of the end zones is the same as for the flanges and so the spring stiffness is the same. At the internal web nodes the spacing is L_2 = (14.400 – 2 x 0.250) / 4 = 3.475 m.

The stiffness of these internal springs in the web wall was:

$$K_2 = k_{mid} L_2 = \frac{0.73G}{1-\upsilon} L_2 = \frac{0.73 \times 10000}{1-0.50} 3.475 = 50{,}735$$

At nodes common to both the web and flange (Numbers 6 and 11 in Figure A8) the external spring stiffness values were summed, so that the value at these locations was 68,300 kN/m.

The gravity load on each spring is calculated by assuming that the wall deforms uniformly. The deflection of each spring is the same and the loads are distributed according to the spring stiffness, as in Equation A2. Table A15 lists the calculations to determine the reaction force at each spring location and the location of the wall centroid.

The wall is symmetrical about the Y axis and so the distance to the centroid is equal to one-half the overall wall depth = 0.5 x 14.400 = 7.200 m. The wall is not symmetrical about the X axis and the centroid is at 5.162 m from node 1, which locates it toward the wall web, as shown in Figure A8.

Table A15. Calculation of U-Shaped Wall Centroid.

	X	y	K	W	Wx	Wy
1	0.13	0.13	34150	88.0	11	11
2	0.13	1.09	24455	63.0	8	69
3	0.13	2.76	24455	63.0	8	174
4	0.13	4.44	24455	63.0	8	280
5	0.13	6.11	24455	63.0	8	385
6	0.13	7.08	68300	176.0	22	1245
7	1.99	7.08	50735	130.7	260	925
8	5.46	7.08	50735	130.7	714	925
9	8.94	7.08	50735	130.7	1169	925
10	12.41	7.08	50735	130.7	1623	925
11	14.28	7.08	68300	176.0	2513	1245
12	14.28	6.11	24455	63.0	900	385
13	14.28	4.44	24455	63.0	900	280
14	14.28	2.76	24455	63.0	900	174
15	14.28	1.09	24455	63.0	900	69
16	14.28	0.13	34150	88.0	1256	11
Sum			603480	1555	11197	8028

$$\bar{x} = \frac{\sum Wx}{\sum W} = 7.200 \qquad \bar{y} = \frac{\sum Wy}{\sum W} = 5.162$$

Step 3: Estimate Period

The rocking periods of the wall in the x and y directions are estimated following the procedure outlined in Figure 5. This requires a single equivalent stiffness and mass value of the

system to be determined. The rocking stiffness of the wall is assembled as the sum of the second moment of area of the stiffness of the individual springs about the calculated centroid. Calculations of the stiffness are tabulated in Table A16. In this table, the adjusted coordinates are calculated as $x' = (x - \bar{x})$ and $y' = (y - \bar{y})$.

Table A16. Calculation of U-Shaped Wall Rocking Inertia.

C	K	x'	y'	Kx'^2	Ky'^2
1	34150	-7.08	-5.04	1709400	866388
2	24455	-7.08	-4.07	1224110	405966
3	24455	-7.08	-2.40	1224110	140787
4	24455	-7.08	-0.72	1224110	12832
5	24455	-7.08	0.95	1224110	22100
6	68300	-7.08	1.91	3418799	249982
7	50735	-5.21	1.91	1378478	185693
8	50735	-1.74	1.91	153164	185693
9	50735	1.74	1.91	153164	185693
10	50735	5.21	1.91	1378478	185693
11	68300	7.08	1.91	3418799	249982
12	24455	7.08	0.95	1224110	22100
13	24455	7.08	-0.72	1224110	12832
14	24455	7.08	-2.40	1224110	140787
15	24455	7.08	-4.07	1224110	405966
16	34150	7.08	-5.04	1709400	866388
Sum				23112564	4138881

This wall has three floors and the equivalent mass is estimated as the mass moment of inertia of the floor mass about the base, as it is calculated in Table A17.

Table A17. Mass Moment of Inertia.

Height, h	Mass, M	Mh^2
10.8	79	9246
7.2	79	4109
3.6	79	1027
Sum	238	14382

The rocking periods of the wall are calculated in each of the two directions as:

$$T_x = 2\pi\sqrt{\frac{M_R}{K_{Rx}}} = 2\pi\sqrt{\frac{14382}{23112564}} = 0.157 \text{ seconds}$$

$$T_y = 2\pi\sqrt{\frac{M_R}{K_{Ry}}} = 2\pi\sqrt{\frac{14382}{4138881}} = 0.370 \text{ seconds}$$

A wall of this configuration was evaluated as part of a separate analysis study and the first two fundamental periods as reported in [8] were 0.352 seconds (X direction) and 0.383 seconds (Y direction). The Y direction periods corresponded closely (0.370 seconds and 0.383 seconds) but the estimated X period of 0.157 seconds was only about one-half the period of 0.352 seconds extracted from the analysis model. This difference can be explained by the eccentricity between the centre of mass and centre of stiffness for deformations in the X direction. This torsional component to the mode shape results in the longer period. This has an impact on the calculated seismic response, as detailed later in this example.

Step 4: Compression Block Size

The length of the compression block is calculated for loads in the X direction by assuming that the neutral axis is in the flange so that the dimension B is the wall flange width of 7.200 m.

$$c = \frac{W}{q_c B} = \frac{1555}{150 \times 7.200} = 1.44\ m < 1.500\ m \quad OK$$

The width of the flange foundation is 1.500 m and the neutral axis depth of 1.440 m is less than this so the assumption of the neutral axis in the flange is confirmed.

For loads in the Y direction the calculation will differ depending on whether the load is in the positive or negative direction. For positive loads, the web will be in compression. As for X loads it is assumed that the neutral axis is within the foundation width (less than 1.500 m) and in this case the width B is assumed to be the web width, 14.400 m:

$$c = \frac{W}{q_c B} = \frac{1555}{150 \times 14.400} = 0.72\ m < 1.500\ m \quad OK$$

When loads are in the negative Y direction the free ends of both flanges are in compression and so the width is the sum of the width of the two foundation beams:

$$c = \frac{W}{q_c B} = \frac{1555}{150 \times (2 \times 1.500)} = 3.456\ m$$

Step 5: Calculate Wall Rocking Strength

The yield force is calculated separately for each direction. For X loads the rocking lateral load is:

$$F_{yX} = \frac{W(\frac{L}{2} - \frac{c}{2})}{\frac{H}{C_0}} = \frac{1555\,(\frac{14.400}{2} - \frac{1.44}{2})}{\frac{10.800}{1.2}} = 1120\ kN$$

For Y direction loads the wall is not symmetrical and so equation 11 is modified depending on the direction of load:

1. Replace $W(\frac{L}{2} - \frac{c}{2})$ *with* $W(L - \bar{y} - \frac{c}{2})$ (*for positive loads*)

$$F_{yY+} = \frac{W(L - \bar{y} - \frac{c}{2})}{\frac{H}{C_0}} = \frac{1555\,(7.2 - 5.162 - \frac{0.72}{2})}{\frac{10.800}{1.2}} = 290\ kN$$

2. Replace $W(\frac{L}{2} - \frac{c}{2})$ *with* $W(\bar{y} - \frac{c}{2})$ (*for negative loads*)

$$F_{yY-} = \frac{W(\bar{y} - \frac{c}{2})}{\frac{H}{C_0}} = \frac{1555\,(5.162 - \frac{3.456}{2})}{\frac{10.800}{1.2}} = 593\ kN$$

The yield coefficient is calculated by dividing the rocking load by the seismic weight of 2,333 kN, which provides an X coefficient of 0.480 and Y coefficients of 0.124 and 0.254 for positive and negative directions of load respectively.

Step 6: Calculate Seismic Displacement

Table A18 implements the same iterative procedure as for the previous examples, where iterations use the average period from the preceding step. In the Y direction, where the response is asymmetrical, the lower of the positive and negative strengths, 0.124, is used to calculate the R factor (e.g.

at step 1, $C(T_1)$=0.701 and R = 0.80 x 0.7013 / 0.1243 = 4.514).

Table A18. Calculation of U-Shaped Wall Effective Period

T_i	$C(T_i)$	R	T_e	T_e/T_i
X Direction Earthquake				
0.157	0.820	1.367	0.214	1.367
0.186	0.820	1.367	0.214	1.155
0.200	0.820	1.367	0.214	1.072
0.207	0.820	1.367	0.214	1.035
0.211	0.820	1.367	0.214	1.017
0.213	0.820	1.367	0.214	1.008
0.213	0.820	1.367	0.214	1.004
0.214	0.820	1.367	0.214	1.002
0.214	0.820	1.367	0.214	1.001
0.214	0.820	1.367	0.214	1.001
0.214	0.820	1.367	0.214	1.000
Y Direction Earthquake				
0.370	0.701	4.514	1.672	4.514
1.021	0.328	2.110	0.781	0.765
0.901	0.360	2.317	0.858	0.952
0.880	0.367	2.359	0.874	0.993
0.877	0.368	2.365	0.876	0.999
0.876	0.368	2.366	0.876	1.000

In the X direction convergence is slow and eleven iterations are required to produce convergence within three decimal places and an effective period of 0.214 seconds. In this direction the period increase is small, from 0.157 seconds to 0.214 seconds, and the response remains on the plateau of the design spectrum.

In the Y direction convergence is faster, and after six iterations the effective period has converged to 0.876 seconds.

At the effective X period of 0.214 seconds the design coefficient C = 0.820. The single degree of freedom displacement is calculated from Equation 13 as

$$\Delta_x = C(T_e)g\frac{T_e^2}{4\pi^2} = 0.820 \times 9810 \times \frac{0.214^2}{4\pi^2} = 9.3\ mm$$

At the effective Y period of 0.876 seconds the design coefficient $C(T_e)$ = 0.368 and the single degree of freedom displacement is:

$$\Delta_y = C(T_e)g\frac{T_e^2}{4\pi^2} = 0.368 \times 9810 \times \frac{0.876^2}{4\pi^2} = 70.2\ mm$$

The top displacement is equal to the calculated spectral displacement times C_0, 9.3 x 1.2 = 11.2 mm in the X direction and 70.2 x 1.2 = 84.2 mm in the X direction.

Step 7: Calculate Ductility Factor

$$DF_x = \frac{C(T_{1x})}{C_{Yx}} = \frac{0.820}{0.480} = 1.7$$

$$DF_y = \frac{C(T_{1y})}{C_{Yy}} = \frac{0.701}{0.124} = 5.65$$

Step 8: Assess Dynamic Amplification Effects on Wall Shear

The dynamic amplification factor is calculated from Equation 19a. From Table 4, the coefficient for a three storey structure is 0.15 and so the omega factor is calculated as:

$$\omega_{VX} = 1 + 0.15 \text{ x } 1.7 = 1.26 \leq 0.5 + N = 3.5$$

$$\omega_{VY} = 1 + 0.15 \text{ x } 5.65 = 1.85 \leq 0.5 + N = 3.5$$

Therefore, the design shear forces are amplified by a factor of 1.26 in the X direction and 1.85 in the Y direction.

The amplification factor is applied to the rocking strength to obtain the design shear force. In the Y direction the strength of the wall differs in the positive and negative direction. Thus the amplification factor is applied to the higher of the two values (290 kN and 593 kN, as calculated above).

Step 9: Calculate Torsional Increase in Displacements

For this wall, the calculated eccentricity is (7.200 – 5.162) = 2.039 m (0.142B) for loads in the X direction and zero for loads in the Y direction, as the wall is symmetrical about the Y axis.

The recommended increase factor for torsion is two times the calculated actual eccentricity, but not less than the accidental eccentricity factor of 0.10. Therefore, displacements are increased by a factor of (1 + 2 x 0.142) = 1.284 in the X direction and by a factor of 1.100 in the Z direction.

Step 10: Assessment of Performance

The maximum X displacement, including the torsion factor, is 11.2 x 1.284 = 14.4 mm and the maximum Y displacement is 84.2 x 1.10 = 92.6 mm.

The height of this wall is 10.800 m and the maximum displacement of 92.6 mm represents a drift angle of 1.2 x 0.093 / 10.800 = 1.03%, much lower than the allowable limit of 2.50%. Therefore, the foundation width of 1.500 m is satisfactory provided the walls design shears are satisfactory:

1 In the X direction, V_x = 1120 x 1.26 = 1,411 kN. This corresponds to an approximate shear stress, based on a shear area of the web wall of $0.80A_g$, of 1411 / (0.80 x 14.400 x 0.250) = 490 kPa.

2 In the Y direction, V_y = 593 x 1.85 = 1,097 kN. The approximate shear stress based on the shear area of the two flanges is 1097 / (0.80 x 7.200 x 2 x 0.250) = 381 kPa.

These shear stresses are within the capacity of a concrete wall with minimum reinforcing.

Comparison with Time History Results

Table A19 compares the design procedure results with the mean results from the time history analysis for the same level of seismic input. As for the preceding examples, the design procedure results were also calculated using the failure soil strength, $2q_c$.

The design procedure values in the X direction showed a wide variation from the time history results. Design displacements were only one-third the time history displacement and the design shear forces were 30% higher. In the Y direction the variation in displacements was much less, within 5%, but the design shears were 30% to 50% higher.

Figure A9 compares the design procedure displacements and base shear coefficients in the X direction with the time history values for all levels of seismic intensity up to ZR = 0.70. This figure shows that the variation generally reduced as the amplitude increased.

Design displacements were 70% lower than the time history results for ZR up to 0.28 but at ZR = 0.70 the difference reduced to less than 20%. Similarly for the base shear coefficient, the discrepancy of 30% at ZR 0.28 reduced to less than 10% at ZR = 0.70.

Table A19. Comparison of Design Procedure Results with Time History Results U-Shaped Wall.

	Displacement Δ (mm)	Base Shear Coefficient, C
X Direction EQ		
Time History Analysis	30.7	0.48
Design Procedure	11.2	0.60
Design Procedure, $2q_c$	10.1	0.63
Z Direction EQ		
Time History Analysis	79.8	0.37
Design Procedure	84.2	0.47
Design Procedure, $2q_c$	78.3	0.56

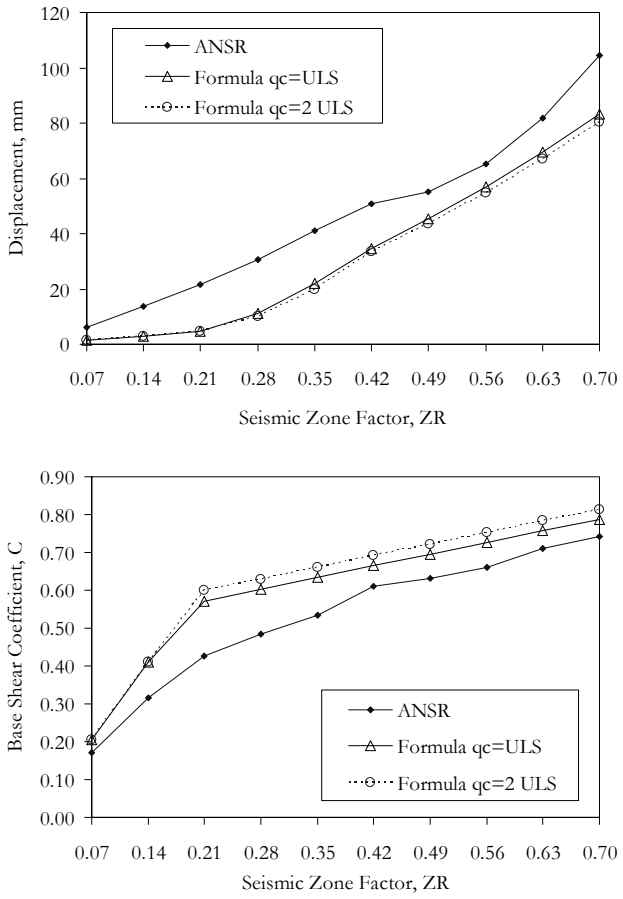

Figure A9. Comparison of (a) Predicted Displacements and (b) Base Shear Coefficient for U-Shaped Wall in the X Direction.

Figure A10 plots a similar comparison of displacements and base shear coefficient versus amplitude for seismic loads in the Y direction. These plots show a good match of displacements between the design procedure and the time history for low to moderate intensity earthquakes, with the variation generally less than 10% up to ZR = 0.49. For higher earthquake intensities the variation increased to as much as 30%. The shear coefficient predicted by the design procedure was consistently higher than the time history, by about 30% up to ZR = 0.28 increasing to 75% higher at ZR = 0.70. The variation was wider when the soil strength of $2q_c$ was used.

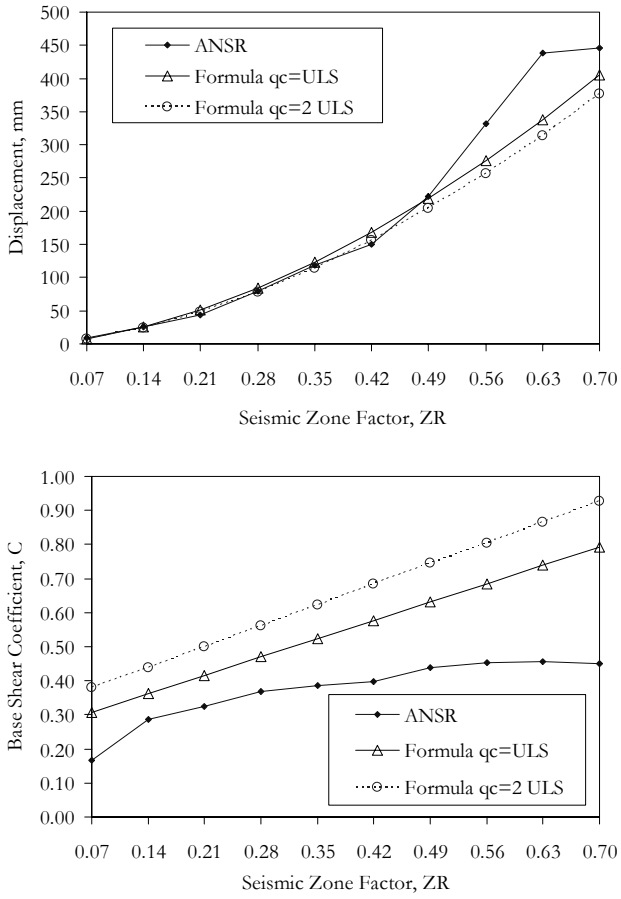

Figure A10. Comparison of (a) Predicted Displacements and (b) Base Shear Coefficient for U-Shaped Wall in the Y Direction.

The main reason for the discrepancy between the time history displacements and the design procedure displacements in the X direction, as shown in Figure A9(a), is that the design procedure used an initial elastic period based on approximate calculations which did not include the effect of the eccentricity in the U-shaped wall. The design procedure values were T = 0.157 seconds, C_m = 0.80 and C_0 = 1.200. The corresponding properties extracted from a finite element analysis were T = 0.352 seconds, C_m = 0.490 and C_0 = 1.284. This shows torsional effects increased the period by a factor of over two and reduced the effective mass factor C_m from 0.80 to 0.49.

Table A19 lists the revised displacements and base shear coefficients calculated using the finite element analysis values as the dynamic parameters. The comparison is plotted in Figure A11. These results show that the use of the more refined parameters considerably improved the correlation of displacements but had little effect on the base shear prediction.

Table A19. Design Procedure X Direction Results Using Modal Analysis Properties.

	Displacement Δ (mm)	Base Shear Coefficient, C
X Direction EQ		
Time History Analysis	30.7	0.48
Design Procedure	28.8	0.62
Design Procedure, $2q_c$	28.8	0.65

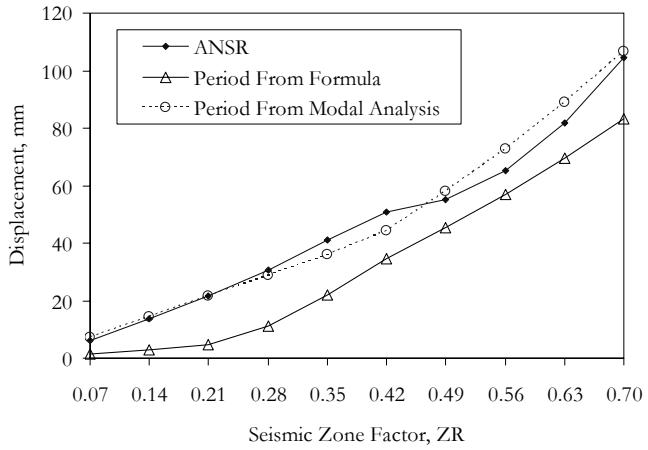

Figure A11. Comparison of (a) Predicted Displacements and (b) Base Shear Coefficient for U-Shaped Wall in X Direction using Modal Analysis Results.

Torsion Displacements

Table A20 lists the displacements at the centre of mass (C of M) and the maximum displacement anywhere on the floor for the analyses with no accidental eccentricity and with the code specified positive and negative eccentricities respectively.

1 In the X direction, the torsional increase in displacements is 39%, which is almost 40% higher than the increase of 28% predicted by the design procedure.

2 In the Y direction the maximum torsional increase in displacements is only 2%, and the configurations with accidental eccentricity actually produce lower maximum displacements than the analysis at the calculated centre of mass. In this direction, the design procedure requires the minimum increase due to torsion, 10%.

Table A20. Torsional Displacements for U-Shaped Wall.

Location	Eccentricity	Displacement	Increase
X Direction			
C of M	None	30.7	
Maximum	None	42.8	39%
Maximum	+ 0.1 B	41.4	35%
Maximum	- 0.1B	42.0	37%
Y Direction			
C of M	None	79.8	
Maximum	None	81.1	2%
Maximum	+ 0.1 B	75.3	-6%
Maximum	- 0.1B	75.3	-6%

The U-shaped wall is loaded eccentrically for loads in the X direction because of the difference in location of the centre of mass and centre of resistance. Figure A12 compares the displacements at the centre of mass (diaphragm node) with the maximum displacement, for both the time history and the design procedure. The design procedure showed a constant increase of 28% at all amplitudes. The time history results showed an increase of approximately 40% for seismic intensities up to ZR = 0.56 but the increase reduced to 16% for the maximum seismic input, ZR = 0.70.

This confirms that the increase in displacement due to torsional effects is not a linear function of drift ratios as implicit in the design procedure but tends to reduce as displacements increase.

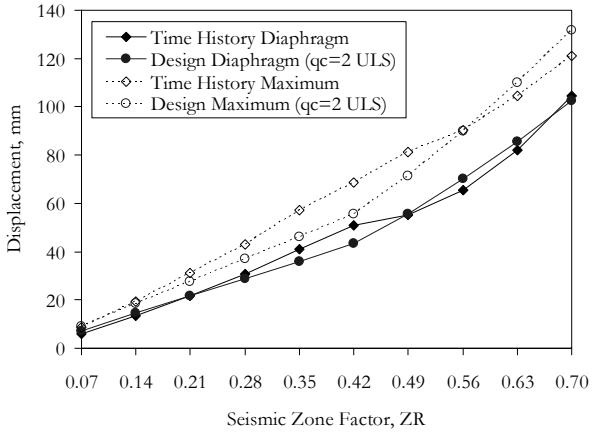

Figure A12. Total Displacements including Torsional Effects for U-Shaped Wall.